

Consistency-Checking 3D Geological Models

Marion N. Parquer¹, Eric A. de Kemp¹, Boyan Brodaric¹ and Michael, J. Hillier¹

Correspondance: Eric A. de Kemp
eric.dekemp@canada.ca
orcid.org/0000-0003-0347-5792

¹Geological Survey of Canada,
Three-dimensional Earth Imaging and Modelling Lab
601 Booth Street, Ottawa, Canada, K0E 1E9

Abstract

3D geological modelling algorithms can generate multiple models that fit various mathematical and geometrical constraints. The results, however, are often meaningless to geological experts if the models do not respect accepted geological principles. This is problematic as use of the models is expected for various downstream purposes, such as hazard risk assessment, flow characterization, reservoir estimation, geological storage, or mineral and energy exploration. Verification of the geological reasonableness of such models therefore is important: if implausible models can be identified and eliminated, it will save countless hours as well as computational and human resources.

To begin assessing geological reasonableness, we develop a framework for consistency-checking with geological knowledge, and test it with a proof-of-concept tool. The framework consists of a space of consistent and inconsistent geological situations that can hold between a pair of geological objects, and the tool assesses a model's geological relations against the space to identify (in)consistent situations. The tool is successfully applied to several case studies as a first promising step toward automated assessment of geological reasonableness.

Keywords – geological knowledge, geological consistency, 3D geological modelling, temporal relation, spatial relation, polarity

1 Introduction

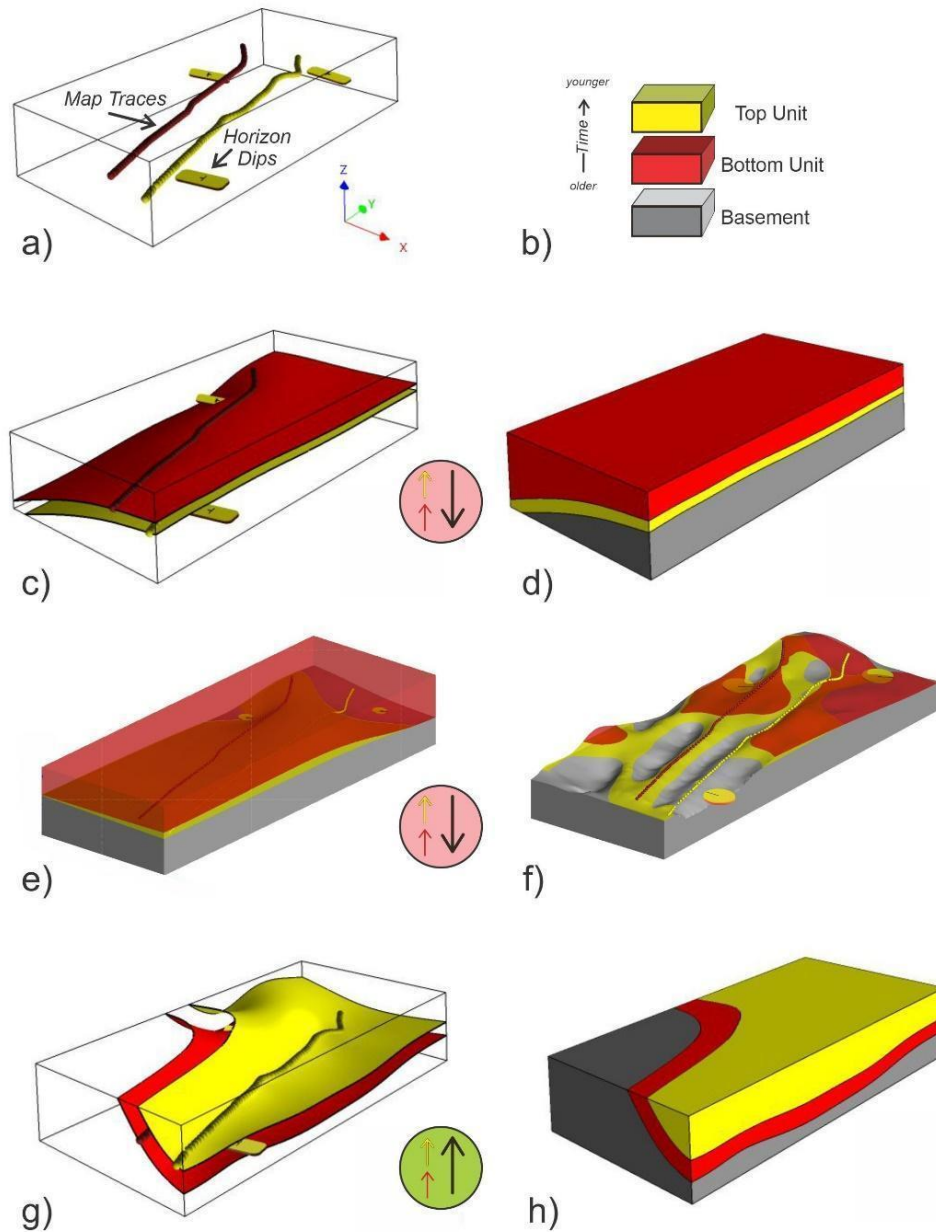
Geomodelling techniques are often deployed to bridge the spatial gaps between explored areas, including gaps in stratigraphic structure, property distribution, and target extent. Increased data availability and rising societal need for natural resources have recently stimulated development of advanced geomodelling modelling techniques such as stochastic simulation (Lajevardi and Deutsch, 2015), time-varying modelling (Hinojosa, 1993), Bayesian techniques (de la Varga and Wellmann, 2016), and direct perturbation of models or data (Lindsay et al., 2012). Wrapped into growing complex workflows (de Kemp, 2016), these new techniques can operate with scarce and heterogeneous data, are frequently deployed to model less accessible and more complex terrains, and often produce a wide range of possible models and associated uncertainties (Wellmann and Caumon, 2018).

1 However, several problems can arise from these advanced techniques. For example, accuracy issues associated with
2 scarce data can occasionally become magnified and lead to geologically questionable spatial interpolations, such as
3 older geological units deposited on younger units (Figure 1). These issues might be further compounded by
4 decreases in the reliability of the data, as the number of participants increases, or by biases at each modelling step
5 (Bond, 2015). Data may also become irrelevant due to scale discrepancies, or degraded due to re-sampling to meet
6 coarser scale requirements or to suit algorithms that imprecisely fit data (Hillier et al., 2021). This can result in
7 various artifacts such as the well-known implicit interpolator ‘bubble’ effect (Frank, 2006; Hillier et al., 2016, 2021;
8 von Harten et al., 2021; Pizzella et al., 2022). As data scarcity and data loss necessarily impact the accuracy and
9 credibility of any model, multiple realizations are often generated in the hope that some model, or the mean of
10 models, comes closer to representing reality and minimizing uncertainty. Many simulations also generate model
11 suites, such as when no priors exist, or when run with the same data or even randomly perturbed data. All these
12 models, however, are not necessarily geologically possible (Deutsch, 2018). Indeed, some of the more data-driven
13 3D modelling methods can generate results that respect the data, but do not necessarily respect established
14 geological principles (Lyell 1833). Conversely, purely knowledge-driven 3D modelling methods might respect
15 geological principles, or ‘norms’, but might not fit the underlying data (Bai et al., 2017). Thus, amongst a multitude
16 of possible models, it is unavoidable that a non-negligible number of them might produce geologically unreasonable
17 results. This is especially a challenge for hypothesis testing, e.g. climate change scenarios, simulated natural
18 systems, or various AI training sets, which might involve billions of such models.

19
20 The highest quality selection from all possible models then must be achieved, or the geological reasonableness of a
21 single model must be assessed. This can be accomplished via some combination of (1) building geologically better
22 models, or (2) excluding inappropriate models. The first solution involves acquiring more and better data,
23 knowledge, or algorithms. Increasing the amount of data, possibly from geophysical or structural measurements
24 (Giraud et al., 2020, 2024; Wellman and Caumon, 2019; Hillier et al., 2014; Grose et al., 2019; de la Varga et al.,
25 2019), or improving data quality, increases overall accuracy and reduces the number of possible models. Similar
26 results also might be achieved with increased knowledge, such as input stratigraphy or augmentation of algorithms
27 with implicit and rule-based approaches (Schaaf et al. 2021, Bertonecello et al., 2013; Bai et al., 2017).

28 Problematically, however, these solutions typically require the acquisition of new data or knowledge, which is often
29 impossible. It also might require the development of more geologically robust algorithms to improve model quality

1 (Jessell et al., 2010; Cherpeau et al., 2010; Ranalli, 1980), such as physics-based modelling approaches (Shokouhi et
 2 al, 2021; Hobbs et al. 2021), which are not yet mature.



3

4 **Figure 1.** Example of *unreasonable* 3D geological models (c) to (f). Sparse input data (a) includes two separate
 5 depositional horizon traces and 3 shallow dipping bedding constraints (yellow-red tablets, yellow is up, red is
 6 down) indicating depositional tops upward. The event history (b) has an older unit (red) deposited below the
 7 younger unit (yellow). However, use of the Lajaunie (1997) implicit method in SURFE (Hillier et al. 2014,
 8 2021) results in the older unit deposited over the younger unit (c)-(d), which is unreasonable in the absence of
 9 other events. Similarly, using commercial software from LeapFrog Geo (Seequent), in (e) without topography
 10 and in (f) with topography, results in an unreasonable geological sequence with the older unit on top and a
 11 miscalculated geological mapping at surface. In contrast, (g) and (h) show reasonable models generated with
 12 SURFE software tuned to respect a minimal horizon thickness and depositional history. Circled arrows show a

1 deposition polarity vector for the older unit (red arrow), younger unit (yellow arrow), and the temporal
2 direction (black arrow, from older to younger unit), as well as the geological plausibility of the situation: a
3 green background indicates consistency with geological principles (aligned vectors), and the red background
4 denotes an inconsistent scenario (unaligned vectors).
5

6 The second solution, which involves model exclusion, can be accomplished manually or automatically: (i) manually,
7 by having a geologist inspect and reject models using accumulated expertise; or (ii) automatically, by performing a
8 rapid computer-driven check to eliminate poor instances, during or after model construction. A significant
9 disadvantage of the manual approach is lack of reproducibility: as expert knowledge can vary between and within
10 geologists (Brodaric *et al.*, 2004; Brodaric 2012, Bond 2015), it is unlikely manual corrections would be
11 reproducible for more than a few models, and the selection of a certain model would likely be unexplainable. The
12 visualization of complex geomodels is a significant challenge, also making manual validation difficult, time-
13 consuming and likely to miss problems. In contrast, if knowledge is made explicit (Brodaric and Gahegan, 2006),
14 automatic approaches could be reproducible and explainable, as per the consistency-checking approach in this paper.
15 Then, a critical aspect of this approach is the explicit digital encoding of knowledge, as well as its integration into
16 geo-modelling workflows. Although integration techniques like rule-based geomodelling (Pyrzcz *et al.*, 2015) and
17 implicit modelling (Jessell *et al.*, 2014) are quite common, they typically incorporate a limited range of knowledge.
18 Extending this range also is not new, e.g. early work focuses on capturing knowledge from a geological map, cross-
19 section, or other field record (Harrap, 2001; Burns, 1975; Burns and Remfry, 1976; Burns *et al.*, 1978; 1969), but
20 only recently have extensions into 3D geo-modelling begun (e.g., Jessell *et al.*, 2021; Rauch, *et al.*, 2019). In
21 addition to limitations in knowledge range, there exist accompanying limitations in its use, as the knowledge is
22 utilized primarily *a priori* for model-building rather than *a posteriori* for model evaluation. Key goals for a
23 consistency checker then include an expansion of the range of knowledge to include an enhanced representation of
24 geological relations, plus an approach for assessing such relations as valid or invalid for effective consistency
25 evaluation.

26
27 A first step to such expansion and evaluation might be the utilization of all information from a geologist's
28 observation sheet. However, it is very unusual to incorporate all such knowledge in a 3D model: much of it remains
29 reported on a map, e.g. as colours, abbreviations or symbols, and the rest in the map legend, in related articles and
30 reports, or in the mind of the geologist. In particular, the geological legend as we know can be incomplete (Harrap,
31 2001) and does not always contain the entire stratigraphic and structural history, prompting the development of a
32 'legend language' as a first attempt to formalize geological map knowledge and check the consistency of traditional

1 2D geological maps (Harrap, 2001). Consistency-checking then involves comparison of relations on a map against
2 the ‘truth’ in a legend; however, legends or other *a priori*/assumed truths, such as stratigraphic columns, might be
3 incomplete, possess errors, or be missing altogether, particularly for under-explored regions such as Mars or many
4 physics-based simulations. Also, it is often difficult to determine if the map or legend is the source of inconsistency.
5 This suggests comparison of a map (or model) against representations of the general rules of geology might be more
6 effective.

7
8 Recent investigations into representing general geological knowledge target the topological aspects of geological
9 maps and models (Schafe et al., 2021; Thiele et al., 2016a, b; Le et al., 2013). These focus on the spatial relations
10 between discrete elements of a 3D model, particularly those unchanging under continuous deformation (Crossley,
11 2005), such as adjacency, inclusion or intersection. An important aspect is the dimensionality of the spatial objects,
12 which might be 0D (a point), 1D (a line), 2D (a surface), or 3D (a volume). These spatial relations are needed for
13 computer encoding to ensure possible object interactions are consistent with, for example, real world physics.
14 Spatial relations between such objects have been widely examined, with distinct relations identified between 2D
15 regions (Egenhofer and Franzosa, 1991) as well as 0D, 1D, 2D, and 3D regions (Zlatanova et al., 2004). They also
16 have been applied to material geological objects (Schetselaar and de Kemp, 2006), providing a basis for the spatial
17 component of geological knowledge, and underpin efforts in knowledge-driven 3D geological model construction
18 (Zhan et al., 2019; 2022). However, they are not yet applied to the evaluation of geological models, especially in
19 combination with temporal relations, despite being applied to the evaluation of models in other domains (e.g. Van
20 Oosterom, 1997; Gong and Mu, 2000; Arora et al., 2021; Nikoohemat et al., 2021; Bezhanishvili et al. 2022).

21
22 In this paper we develop a general framework for consistency-checking 3D geological models, a proof-of-concept
23 consistency-checking tool, and test a portion of the framework using the tool in four case studies. The framework
24 consists of a hyperspace of all possible (in)consistent geological relations holding between nine kinds of geological
25 objects, with each relation being a unique combination of a spatial, temporal and polarity relation. The proof-of-
26 concept tool then assesses the relations in the case-studies against a subspace involving four kinds of objects - i.e.
27 depositional and intrusion units, and fault and erosional surfaces - to successfully identify (in)consistencies.
28 Although testing of the full hyperspace, involving all nine object types, is left to future work, the overall framework
29 seems promising and performs as expected on the case studies. The framework is presented in Section 2, the tool is

1 described in Section 3, the four case studies are presented in Section 4, some additional thoughts on consistency-
2 checking and geological reasonableness are presented in Section 5, and the paper concludes with a brief recap in
3 section 6.

4

5 **2 Geological Consistency-Checking Framework**

6 Geological data and knowledge have been accumulated over thousands of years of human inquiry into our natural
7 environment, with modern formal geological knowledge emerging in the mid 1800's (Lyell 1833; Rothery, 2016). A
8 collective understanding is found in digitally archived articles and books (e.g. Kardel and Maquet, 2012), in online
9 products and courses (e.g. Fattah, 2018), and in several formal ontological articulations (Brodaric and Richard 2021,
10 Garcia et al. 2020, Perrin et al. 2011, Brodaric, B. and Gahegan 2006). It is particularly useful to help understand the
11 often hidden and unobserved subsurface of the Earth. However, the various possible sources of data (e.g. surface
12 mapping, boreholes, geophysical surveys) generally cannot provide sufficiently uniform and continuous information
13 for a volume of interest. Supplementary geological knowledge is required for improved interpretation between
14 sometimes extremely scarce observations (Groshong, 2006; Frodeman, 1995), especially when coupled with new
15 data integration techniques and approaches (Giraud et al. 2020; Wellmann and Caumon, 2018).

16

17 For consistency-checking purposes herein, we distinguish between data and knowledge, with data being
18 observational, and geological knowledge being either local or universal. Data then includes any form of observation
19 used to understand a specific geological situation, e.g. bedding top indicators, structural orientations, fault and
20 horizon contacts, seismic picks, or other geophysical readings. Local knowledge applies to a specific area but is not
21 observational: it is interpretational and includes things such as the local stratigraphy and process history. In contrast,
22 universal geological knowledge is applicable to different geographical areas and includes things such as general
23 laws, principles, process types, and classification systems, e.g., Walther's Law, uniformitarianism, the notion of
24 deposition, rock type classification. Significantly, data and knowledge are interconnected insofar as knowledge is
25 inferred from data, and the data is contextualized by knowledge during observation and interpretation (Brodaric et
26 al, 2004). Indeed, both data and knowledge are required to arrive at any interpretation, including a 3D geo-model.
27 Consistency then can be seen as the degree of agreement between a model and the relevant data and knowledge.
28 However, current modelling techniques are primarily focused on ensuring and assessing data consistency, with
29 knowledge consistency less developed, e.g. implicit modeling techniques typically optimize fit to data and assume

1 stratigraphic consistency, but such consistency might not be achieved by all techniques (see Figure 1), and further
2 might not be reflected in all geometric realizations due to idiosyncrasies of spatialization algorithms (Hillier et al.,
3 2021). Therefore, some output geological models can still fail to respect basic geological principles.

4

5 To determine knowledge consistency for a 3D geo-model, we expect local knowledge to be typically derived from a
6 2D map legend, cross-section, or associated report, with the geological processes and the combined event histories
7 being discerned through geologically possible binary relations. For example, the contact relation between two
8 adjacent depositional units can be decomposed into a spatial relation (spatially touching), a temporal relation
9 (temporally adjacent), and polarity relations (aligned material gain or loss), and each of these can be evaluated
10 separately for consistency with established geological knowledge.

11

12 CC Truth Tables, or consistency checking truth tables, then denote all possible combinations of these relations for
13 pairs of object types, with each combination identified as (in)consistent. Knowledge consistency is finally assessed
14 by traversing the spatial relations between pairs of objects in a geo-model, using the local knowledge to determine
15 object types, temporal relations, and polarities of the objects, which together form an index into the truth table,
16 which denotes universal knowledge, to determine the (in)consistency of a specific relation.

17

18 **2.1 Geological Objects and Polarity**

19 The geological objects in a 3D geo-model (geo-objects) are, for the purposes of this paper, representations of
20 instances of nine distinct geological object types: depositional unit, intrusion unit, extrusion unit, metamorphic unit,
21 fault, erosion surface, fold volume, and linear and planar fabric. This list is not comprehensive, but reflects an initial
22 suite of key entity types found in models.

23

24 Each geo-object is either material or immaterial. A material geo-object is constituted by some rock material and is
25 volumetric as it occupies 3D space. An immaterial geo-object is not constituted by any rock material, but (1) might
26 be volumetric and occupy 3D space, such as a fold which occupies the space of its host rock, or (2) is not volumetric
27 and occupies lower-dimensional space, such as a 2D fault or erosional surface. Note that horizons, understood as
28 the top or bottom surfaces of a volume, are excluded from the geological object types primarily because, in effect,
29 they imply a volume and are thus already incorporated into the volumetric types. This does not exclude the top or

1 bottom surfaces of material entities from being represented in 3D geo-models, but they are not distinct geological
2 object types in this paper and are converted to 3D volumes for consistency-checking in our proof-of-concept tool.
3

4 Additionally, we utilize two types of polarity associated with geological objects: internal polarity and temporal
5 polarity. Internal polarity is a vector within a geo-object roughly pointing in the direction of creation or destruction
6 of the object's material, or in the growth direction of the object's boundary: e.g. for depositional units, from the base
7 or oldest part of the geological body to the top (in the direction of material accumulation), for erosional surfaces
8 from the top to bottom of the eroded rock body (in the direction of material destruction), and for igneous units from
9 the core to the distal geological contacts with host rocks (in the direction of boundary change). Although material
10 geo-objects generally possess a global internal polarity, some immaterial geo-objects of lower-dimensionality lack
11 polarity as they are not associated with material growth or destruction, e.g. fault surfaces, while other immaterial
12 geo-objects, such as an erosion surface, possess an internal polarity pointing in the direction of material destruction
13 of the eroded unit.
14

15 Geo-objects also might have many local internal polarities distributed throughout the object, constituting an internal
16 polarity field and forming the basis for determining its global polarity. Significantly, although we strictly use global
17 polarity in this paper, the overall framework developed herein does not depend on it and would equally function
18 with local polarities. Note there are pros and cons associated with each type of polarity. Although data for global
19 polarity is generally more available and easier to implement in tools, it could be hard to estimate in certain
20 situations, e.g. radial cooling directions for intrusions in which a single vector trend does not suffice. In contrast,
21 local polarities are often difficult to obtain and harder to implement in automated tools.
22

23 Temporal polarity is an age direction vector that represents an oriented age relation held by two geo-objects,
24 pointing from the older to the younger object and set parallel to one of the object's internal polarity. As a vector, and
25 in contrast to a typical relation, it orients the age relation in space, thus enabling comparison with internal polarity
26 vectors as well as direction-oriented space-time analysis of geo-object interactions. Collectively, there can exist
27 three polarity vectors associated with a pair of geo-objects: the internal polarity of each object and the temporal
28 polarity holding across the objects. The alignment of these vectors then helps determine the geological plausibility
29 of the situation (see Figure 1). The nine types of geo-objects, and associated polarities, include:

1
2
3
4
5
6
7
8
9
10
11
12
13
14
15
16
17
18
19
20
21
22
23
24
25
26
27
28
29

- Depositional unit: a material rock volume formed primarily by processes like gravity, water, or air transporting and accumulating materials over a specific time interval. The internal growth direction of this unit is mainly vertical and points upward, from the bottom to the top of the unit, opposite to the force of gravity at the time of deposition (Figure 2a). Although these units can extend laterally over a large area, their formation is driven by near-vertical deposition.
- Extrusion unit: a material rock volume primarily generated by igneous extrusive processes and associated with a time interval. The local internal polarities typically point radially upwards to a proximal vent or feeder facies. This includes internal polarities associated with deposition of eruptive material, which is affected by gravity and tends to flow downhill, but with airfall material accumulating upward. A global internal polarity vector thus points upwards at the time of formation, similar to sedimentary units. However, extrusive units with variable growth direction, such as in subglacial situations are an exception, having chaotic eruptive depositional internal polarity vectors that cannot be characterized by a single global vector; a global internal polarity vector thus would be absent for such units.
- Intrusion unit: a material rock volume primarily generated by igneous subterranean processes and associated with a time interval. Its internal polarities radiate from a core region towards the cooling host rock contact surfaces (Figure 2c), with a global internal polarity set to a representative direction. This polarity can be seen as boundary growth - the growth direction of the boundary of the unit - often in opposition to material accumulation as intrusions tend to have new material added to their core. Many configurations for the growth gradients in these bodies exist, but in general the emplacement contacts with host rocks are similar to unconformities, in that they tend to be truncating earlier material through magmatic erosion, assimilation or expansion (Annen, 2011).
- Metamorphic unit: a material rock volume primarily generated by deep thermal-kinetic-chemical processes and associated with a time interval. The internal polarities are perpendicular to the metamorphic isograd and point to the lower metamorphic grade or into the host protolith (Figure 2d). In many cases a global internal polarity vector can be set pointing upwards from a core heat source. This holds for a regional perspective, in which we can envision the earth's regional geothermal gradient as pointing from hotter-deeper to cooler-shallower lithospheric material. It also holds for a local perspective, in which the location of the source of metamorphism, and hence the local gradient, may be easier to establish from metamorphic

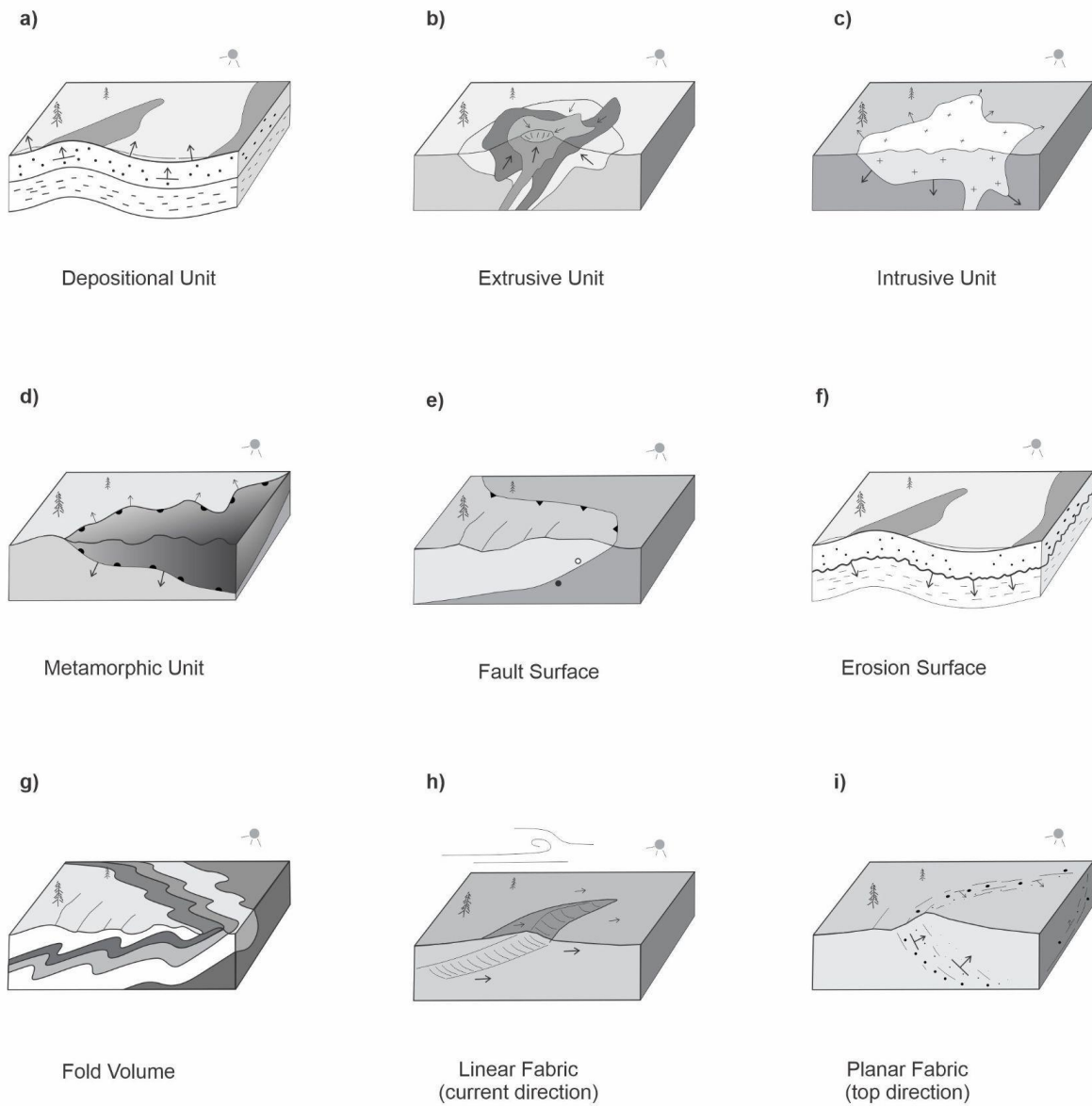
1 aureoles around intrusions. The metamorphic unit geo-object is included herein to allow analysis of
2 thermal-kinetic-chemical gradients with respect to other related geological features.

- 3 ● Fault surface: an immaterial 2D surface between displaced rock volumes that were once continuous, and
4 associated with a time instant or interval for the displacement activity (Figure 2e). The surface lacks
5 internal polarity, as it is never constituted by any material. Fault surfaces are distinguished from fault
6 blocks or zones (Qu et al. 2023), with the latter material and volumetric, but not considered in this paper.
- 7 ● Erosion surface: an immaterial 2D surface where a rock volume has completely or partly eroded via a
8 mechanical or chemical process. It is associated with a time interval or instant indicating the end of the
9 erosion process. Its global internal polarity points in the direction of material destruction (Figure 2f).
- 10 ● Fold: the shape of the underlying host rock often caused by various tectonic and/or gravity-driven processes
11 within a time interval (Figure 2g). Because shape is a characteristic (or property) of its host, like colour,
12 size or thickness, it cannot be a material entity, so folds are immaterial. Such characteristics also are not
13 parts of their host: a rock unit's characteristics such as shape, colour, or thickness are not a fragment of the
14 unit. The host, however, might be either material or immaterial: host rock units are material, but host faults
15 or erosional surfaces are immaterial. As folds occupy the space of their host, they further can be volumetric
16 or lower-dimensional. Herein we consider folds as immaterial objects without internal polarity, but they
17 might have a form of kinematic polarity, such as vergence and tectonic transport direction, which we do not
18 address in this work.
- 19 ● Linear fabric: a penetrative linear orientation of some rock material with an associated time interval.
20 Specifically, the fabric is a whole with its material parts aggregated in a linear orientation, thus the fabric is
21 material and volumetric. Some linear fabrics could have a unidirectional global internal polarity (Figure
22 2h), such as from paleocurrents, or a bidirectional global internal polarity, such as from tidal currents.
- 23 ● Planar fabric: a penetrative planar orientation of some volumetric rock material parts, with an associated
24 time interval. A primary planar deposition fabric has a positive upward polarity at the time of formation
25 (Figure 2i), (i.e., bedding top observations). A metamorphic planar fabric in general has no polarity.
26 Igneous fabrics might have an internal polarity direction from crystal accumulation, igneous flow layering,
27 or emplacement contact directions. Fabrics in general are key to resolving complex event histories (Burns
28 1988). As all fabrics are composed of materials arranged in a certain spatial orientation, and these materials
29 are part of a host rock unit, then fabrics are also a material part of their host. This differentiates fabrics from

1 folds in this paper: in contrast to fabrics, folds are composed of shapes that are immaterial characteristics,
2 not parts, of their host.

3

4 Field geologists typically infer these geo-objects, and associated geological histories, by interpreting repeated
5 geological relations across field sites, suggesting the presence of a simple topological framework underlying
6 variously complex geological situations. Such relations further can be decomposed into combinations of spatial,
7 temporal, or polarity relations. For example, if depositional unit Sandstone-A is *intruded-by* intrusion unit Granite-
8 B, then we also expect a spatial relation to hold such as Sandstone-A *spatially meets* Granite-B, a temporal relation
9 to hold such as Sandstone-A *is temporally met by* Granite-B, and the global internal polarities are either *aligned* or
10 *opposed*. A consistency checker then must verify the validity of such relation combinations.



1

2 **Figure 2.** Examples of geological objects with polarities, symbolized with black arrows. Metamorphic unit (d) is a
 3 contact aureole around an intrusion, isograds ornamented on the warmer side. Note fault features do not have
 4 internal polarity (e). Planar depositional point observations depicted in (i).

5

6

7

1 **2.2 Spatial Relations**

2 Prominent formalisms for binary spatial relations are derived from two main approaches (Galton 2009), Region
 3 Connection Calculus (RCC) and the 9-intersection model (9I; Egenhofer, 1989; Egenhofer et al., 1993, Egenhofer
 4 and Franzosa, 1991). In this paper we informally adapt the 9I approach , implemented for 0, 1, 2 or 3D objects and
 5 512 possible spatial relations (Zlatanova et al., 2004). However, these 512 possibilities are drastically reduced for
 6 typical geological situations in 2D and 3D (Schetselaar and de Kemp, 2006), resulting in 40 spatial relations for the
 7 nine geological object types, as shown in Figure 2; then for any pair of spatial objects only one spatial relation can
 8 hold. These relations can be represented as a three-part tuple, as shown in Tuple Equation 1. The tuple is also
 9 directed or not, depending on the symmetry of the relation, given that asymmetric relations are directional and
 10 symmetric relations are not directional; e.g. *meets* is symmetric, so if A *meets* B then B meets A, thus *meets* is not
 11 directional; but if A *contains* B then it cannot be the case that B *contains* A (or A *is contained by* B), so *contains* is
 12 asymmetric and directional. The symmetric spatial relations from Table 1 are *is disjoint with*, *meets*, *overlaps*,
 13 *equals*, *intersects*, and the remaining relations are asymmetric. Symmetric relations also are their own converse,
 14 whereas asymmetric relations have distinct converses, such as A *contains* B and B *is contained by* A.

15
16

$$\text{Entity}_A \left\{ \begin{array}{l} \textit{is disjoint with} \\ \textit{meets} \\ \textit{overlaps} \\ \textit{contains} \\ \textit{is contained by} \\ \textit{covers} \\ \textit{is covered by} \\ \textit>equals} \\ \textit{intersects} \end{array} \right\} \text{Entity}_B \quad (1)$$

17
18

| Spatial Relations | 3D/3D | 3D/2D | 3D/1D | 2D/2D | 2D/1D | 1D/1D |
|----------------------|-------|-------|-------|-------|-------|-------|
| A is disjoint with B | | | | | | |
| A meets B | | | | | | |
| A overlaps B | | | | | | |
| A contains B | | | | | | |
| A is contained by B | | | | | | |
| A covers B | | | | | | |
| A is covered by B | | | | | | |
| A equals B | | | | | | |
| A intersects B | | | | | | |

1
2
3
4
5
6
7
8
9

Table 1. The 9 spatial relations between two geological objects of 1/2/3 dimensions. Blank gray cells denote impossible spatial relations; after Egenhofer (1989), Egenhofer et al. (1993), Egenhofer and Franzosa (1991), and Zlatanova et al. (2004).

1 **2.3 Temporal Relations**

2 Temporal relations are required to establish a temporal ordering between geological objects (Perrin et al., 2011).
 3 Though the temporal position of a geological object is not always known (Michalak, 2005), the temporal ordering
 4 between objects can be derived from the timeline of associated generative events (Galton, 2009; Claramunt and
 5 Jiang, 2001). As with spatial relations, dimensionality plays a role: temporal relations can be categorized according
 6 to the nature of the time duration (of the event) with 3 potential combinations: period/period, period/instant, or
 7 instant/instant. Building on Allen’s definitions (Allen, 1983), this leads to 14 distinct temporal relations, including
 8 converses (e.g. *A precedes B* and *B is preceded by A*), as shown in Table 2, for the nine geological object types;
 9 moreover, for any pair of objects only one temporal relation can hold. Of note is the *is incomparable to* relation,
 10 which indicates the temporal ordering is unknown due to unavailable temporal knowledge about one or both objects.
 11 Though instantaneous event durations are unlikely in reality, they are common in recorded knowledge and data, thus
 12 time instants are valuable to the framework. Tuple Equation 2 illustrates the three-part tuple for expressing these
 13 relations. The symmetric relations are *equals* and *is incomparable to*, with the remainder being asymmetric.

14

$$\begin{array}{c}
 \left. \begin{array}{l}
 \textit{Entity}_A
 \end{array} \right\} \begin{array}{l}
 \textit{precedes} \\
 \textit{meets} \\
 \textit{overlaps} \\
 \textit{is finishedby} \\
 \textit{contains} \\
 \textit{starts} \\
 \textit>equals} \\
 \textit{isincomparableto} \\
 \textit{isstartedby} \\
 \textit{isduring} \\
 \textit{finishes} \\
 \textit{isoverlappedby} \\
 \textit{ismetby} \\
 \textit{isprecededby}
 \end{array} \left. \begin{array}{l}
 \textit{Entity}_B
 \end{array} \right\} \quad (2)
 \end{array}$$

15

16

17

18

| temporal relations | period / period | period / instant | instant / instant |
|--|-----------------|------------------|-------------------|
| <i>A precedes B</i> <i>B is preceded by A</i> | | | |
| <i>A meets B</i> <i>B is met by A</i> | | | |
| <i>A overlaps B</i> <i>B is overlapped by A</i> | | | |
| <i>A starts B</i> <i>B is started by A</i> | | | |
| <i>A finishes B</i> <i>B is finished by A</i> | | | |
| <i>A during B</i> <i>B contains A</i> | | | |
| <i>A equals B</i> | | | |
| <i>A is incomparable to B</i> | | | |

1

2

Table 2. The 14 temporal relations between two geological objects, after Allen (1983). The temporal timeline advances from left to right in each cell. Blank gray cells denote impossible temporal relations, and blank white cells denote unknown temporal relations.

3

4

5

6

7

8

9

2.4 Polarity Relations

10

A polarity relation can be determined from up to three independent component polarities (discussed earlier in

11

12

Section 2.1): the two internal polarities, dependent on the type of geo-object and its creation processes, and the

13

temporal polarity. The internal and temporal polarity vectors can be compared to determine if they are ‘aligned’ or

14

‘opposed’:

15

- Aligned polarity relation: the vectors are roughly parallel, such that each vector is within 90° of every other vector.

16

17

- Opposed polarity relation: a vector is oriented in an opposite direction to the others, such that one vector is at least greater than 90° from one of the others.

18

19

Importantly, polarity alignment or opposition does not necessarily determine (in)consistency alone, as such

20

determination requires consideration of the spatial and temporal relations. For example, opposed internal polarity

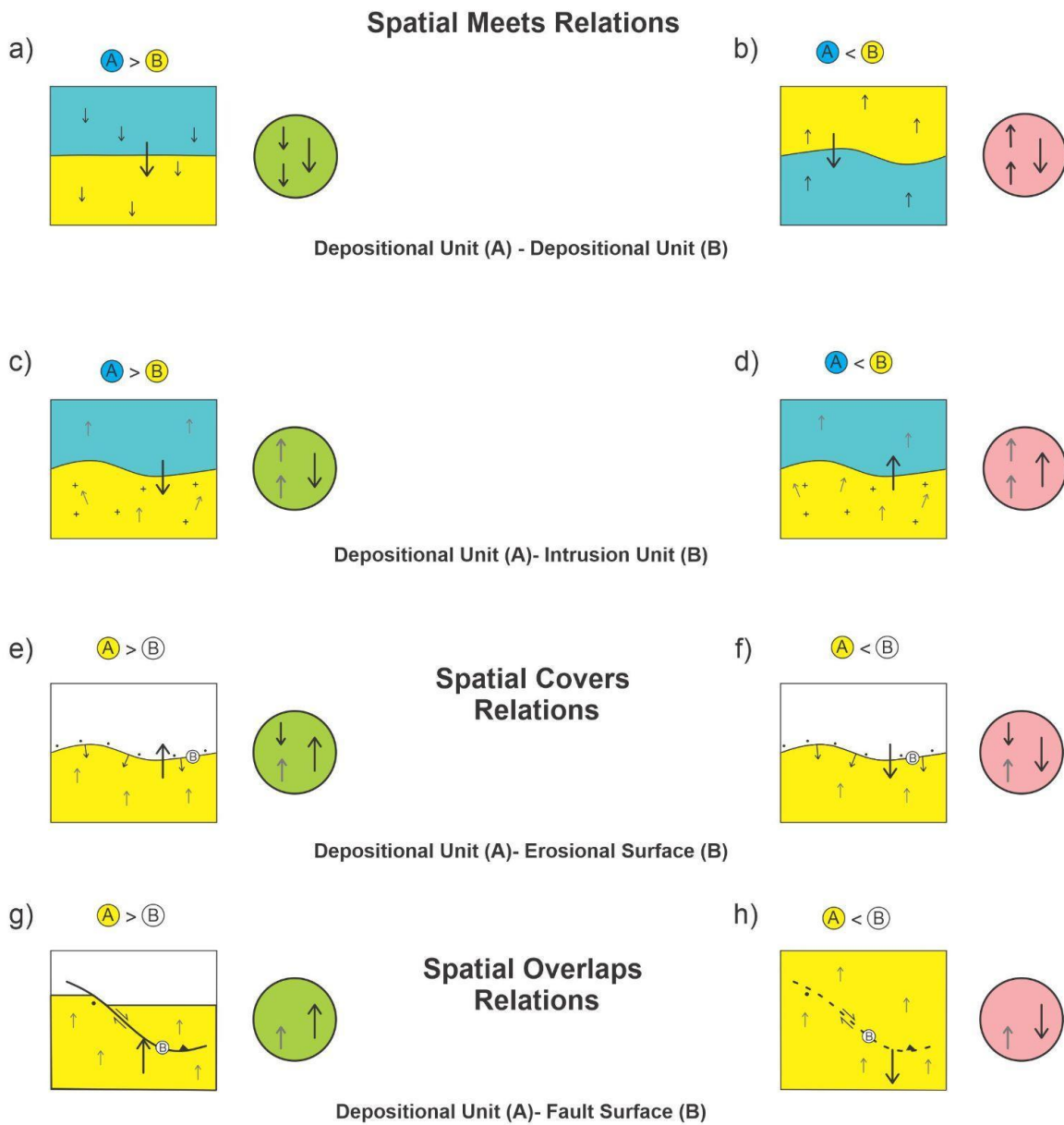
21

can indicate either inconsistency or consistency: e.g. depositional units that spatially meet and have opposed internal

1 or temporal polarities are inconsistent (Figure 3b), because such units must create material in the same spatial and
2 temporal direction; but a touching depositional unit and erosional surface with opposed internal polarity are
3 consistent, because the surface must erode material towards the older unit (Figure 3e). The internal polarity relation
4 also might not play a determining role in assessing (in)consistency, as the spatial and temporal relations may
5 individually or together be determining factors: e.g. the (in)consistency of an intrusion into a host depositional unit
6 is determined regardless of internal polarity (Figure 3c-d), as the intrusion must be younger and touching the unit,
7 otherwise some interceding object such as a fault or erosional surface is missing from the model; similarly for a
8 depositional unit and a fault surface (Figure 3g-h), as the unit must pre-exist the fault. Note we do not consider
9 growth faults to be strictly synchronous within a full unit, since at least some of the material needs to be in place
10 first, prior to faulting. Additional examples of consistency-checking with polarities are shown in Appendix 2.

11
12 The requirement for this complex polarity relation might not be intuitive, but it is driven by the need for wide
13 applicability across diverse geological situations and knowledge environments. Immediate simplifications are
14 limited and do not generalize. For example, checking a model solely against *a priori* local knowledge is not always
15 possible, due to its incompleteness, incorrectness, or absence, and related sources of inconsistency - model or
16 knowledge - are often indeterminate. The temporal polarity relation alone also is insufficient: e.g. even in simple
17 depositional environments, consistency assessment requires knowledge of spatially above and below relations -
18 younger units are above older units - and these spatial relations are typically hard to determine computationally.
19 Moreover, such simplifications fail in complex geological situations: e.g. spatially above and below cannot be
20 determined for a depositional unit pair stacked side-by-side, perhaps due to tectonism; and the temporal vector on its
21 own cannot discriminate the valid and invalid spatial configurations for this pair, but these can be resolved with the
22 polarity relation.

23
24 A general framework for (in)consistency therefore must take into account the spatial, temporal, and polarity
25 relations. This is accomplished by using these relations as an index into truth tables representing geological norms
26 and specifying the (in)consistency of the situation (see Section 2.5).



1

2 **Figure 3.** Examples of consistent (green circle) and inconsistent (red circle) polarity configurations for the spatial
 3 *meets*, *covers* and *overlaps* relations, and for the temporal *meets* relation, e.g. $A > B$ is A temporally *meets* B,
 4 and $A < B$ is A *met by* B; included are two vectors for internal polarity (small arrows) and a third vector for
 5 age polarity pointing from older to younger object (large arrow); top small arrow in circle is for A, and bottom
 6 is for B. For the two depositional units depicted in (a), the entire package is overturned by a later process, but

1 nevertheless is consistent. This would still be the case if the package of units is rotated by any angle, including
2 vertically where there would be no sense of relative below and above for the units. An inconsistent scenario
3 between such units is depicted in (b), as the age polarity is opposed to one of the internal polarities, implying
4 reverse deposition of older on younger material. In (c) the deposition - intrusion unit scenario is consistent, as
5 the age vector is aligned with the intrusive process, whereas in (d) it is not allowed because the host
6 depositional unit is younger than the intrusion unit. In both (c) and (d) the internal polarities do not impact
7 consistency evaluation, as age is the determining factor. In (e) and (f) the erosional surface needs a pre-
8 existing material to erode, thus the direction of material reduction of the eroding surface moves into the older
9 underlying depositional material. For a consistent scenario the age vector points from the older unit to the
10 younger erosional surface (e), and for an inconsistent scenario, the age vector points from the older surface to
11 younger unit (f), with only 2 opposing polarity vectors needed to determine validity, age vector and erosion
12 direction. In (g) the fault has no internal polarity, but needs a material object to displace. When the
13 depositional unit pre-exists, as in (g), the relation is valid; however, in (h) the depositional unit is younger and
14 did not exist when the fault evolved, so the relation is inconsistent. Grayed arrows indicate the internal
15 polarity vector is not essential for truth table consistency.
16

17 **2.5 Geological Principles**

18 Many geological principles, known implicitly to geologists, must be considered in assessing, even grossly, the
19 consistency of the spatial, temporal, and polarity relations between two geological objects (Ziggelaar, 2009; Aubry
20 et al., 1999). Amongst the foremost are the following considerations:

- 21 ● principle of lateral continuity: in general, a given depositional unit tends to have a similar age over its
22 full extent. Diachronous and heterochronous units are not uncommon.
- 23 ● principle of actualism: past objects are formed by processes (tectonism, magmatism, deposition ...)
24 acting in the same way as today.
- 25 ● principle of paleontological identity: two objects with the same association of stratigraphic fossils are
26 considered contemporary.
- 27 ● principle of superposition: without structural disruption events, a given object is younger than the
28 object it overlies and older than the one overlying it.
- 29 ● principle of horizontality: sedimentary objects, have initial nearly horizontal orientation; a non-
30 horizontal sedimentary sequence is generally deformed after its deposition with faulting, slumping or
31 tectonic folding. Local exceptions occur such as syn-sedimentary deformation.
- 32 ● principle of cross-cutting: a given material layer is older than objects cross-cutting it.
- 33 ● principle of inclusion: an object included into another object is older than the including object (clasts in
34 a conglomerate or a volcanic flow picking up older material), except when a younger object internally
35 displaces the enclosing object (i.e. geode, dyke, sill, migmatite melt phase).

36

1 For the nine types of geological objects considered herein, 45 valid pairwise combinations of objects are possible,
2 but this paper focuses on 7 key tables and subspaces relevant to the case studies (see Code and Data Availability).
3 For each object combination, a ternary CC Truth Table establishes all possible consistent and inconsistent spatial-
4 temporal-polarity relations between the geo-object types: spatial relations along one side, temporal relations along
5 another side, and internal polarities along a third side; each table cell then can be marked as consistent or
6 inconsistent for the pair of objects. Alternatively, the truth tables can be seen as denoting a five-dimensional
7 hyperspace representing all possible geological relations, with axes corresponding to two geo-object types and their
8 spatial, temporal, and polarity relations. Values along the axes are the discrete relation types, e.g. the spatial axis has
9 values for *is disjoint with*, *meets*, etc. Consistent values are objects in this space, while inconsistent values occupy
10 empty points in the space. For example, a consistent object might be found at (*depositional unit, depositional unit,*
11 *spatial meets, temporal meets, aligned*), but the space is empty and inconsistent at (*depositional unit, depositional*
12 *unit, spatial meets, temporal precedes, aligned*). When polarity is irrelevant, the cell values are the same for both
13 aligned and opposed rows, leaving the polarity subspace empty and set to null. For instance, (*depositional unit,*
14 *intrusion unit, spatial meets, temporal meets, null*) is consistent when the depositional unit is older than the intrusion
15 unit it touches. Note the polarity axis remains necessary for the other cases in which polarity co-determines
16 consistency.
17

| | | TEMPORAL RELATIONS | | | | | | | | POLARITY | |
|-------------------|----------------------|--------------------|-----------|--------------|--------------------|--------------|------------|------------|------------------------|---------------|---------------|
| | | A precedes B | A meets B | A overlaps B | A is finished by B | A contains B | A starts B | A equals B | A is incomparable to B | | |
| SPATIAL RELATIONS | A is disjoint with B | Green | Green | Green | Green | Green | Green | Green | Green | ↑↑ aligned ↓↓ | ↑↓ opposed ↑↓ |
| | A meets B | Green | Green | Green | Green | Green | Green | Green | Green | ↑↑ aligned ↓↓ | ↑↓ opposed ↑↓ |
| | A overlaps B | Green | Green | Green | Green | Green | Green | Green | Green | ↑↑ aligned ↓↓ | ↑↓ opposed ↑↓ |
| | A contains B | Green | Green | Green | Green | Green | Green | Green | Green | ↑↑ aligned ↓↓ | ↑↓ opposed ↑↓ |
| | A is contained by B | Green | Green | Green | Green | Green | Green | Green | Green | ↑↑ aligned ↓↓ | ↑↓ opposed ↑↓ |
| | A covers B | Green | Green | Green | Green | Green | Green | Green | Green | ↑↑ aligned ↓↓ | ↑↓ opposed ↑↓ |
| | A is covered by B | Green | Green | Green | Green | Green | Green | Green | Green | ↑↑ aligned ↓↓ | ↑↓ opposed ↑↓ |
| | A equals B | Green | Green | Green | Green | Green | Green | Green | Green | ↑↑ aligned ↓↓ | ↑↓ opposed ↑↓ |
| | A is disjoint with B | Red | Red | Red | Red | Red | Red | Red | Red | ↑↑ aligned ↓↓ | ↑↓ opposed ↑↓ |
| | A meets B | Red | Red | Red | Red | Red | Red | Red | Red | ↑↑ aligned ↓↓ | ↑↓ opposed ↑↓ |
| | A overlaps B | Red | Red | Red | Red | Red | Red | Red | Red | ↑↑ aligned ↓↓ | ↑↓ opposed ↑↓ |
| | A contains B | Red | Red | Red | Red | Red | Red | Red | Red | ↑↑ aligned ↓↓ | ↑↓ opposed ↑↓ |
| | A is contained by B | Red | Red | Red | Red | Red | Red | Red | Red | ↑↑ aligned ↓↓ | ↑↓ opposed ↑↓ |
| | A covers B | Red | Red | Red | Red | Red | Red | Red | Red | ↑↑ aligned ↓↓ | ↑↓ opposed ↑↓ |
| | A is covered by B | Red | Red | Red | Red | Red | Red | Red | Red | ↑↑ aligned ↓↓ | ↑↓ opposed ↑↓ |

1
2
3
4
5
6
7
8
9
10
11
12

Table 3. CC Truth Table showing consistent (green) and inconsistent (red) spatial-temporal-polarity relations between two depositional units. All 14 temporal relations are not included (as columns) as the values are duplicated for the inverse temporal relations.

The CC Truth Table in Table 3 illustrates all possible spatial-temporal-polarity relation combinations for two depositional units. The eight columns represent the temporal relations possible between two intervals of time; the remaining inverse temporal relations are excluded for reasons of space and redundancy, as the values in each row are repeated for the temporal inverse, e.g. *A precedes B* and *A is preceded by B* are both red. The rows in a truth table represent the possible spatial and internal polarity relations between two depositional rock volumes. Green cells then indicate consistent combinations, red cells inconsistent combinations, with the consistent cells being far less numerous. Indeed, in Table 3, two distinct depositional units can be spatially related only via *is disjoint with* or

1 *meets*, once material sharing is excluded (see assumptions below). All combinations are possible for spatially
2 disjoint units, but only aligned polarity is valid for units that spatially meet, because opposed polarities would signal
3 inconsistencies, such as missing events or intermediary objects. As the truth tables are not necessarily columnar
4 symmetric, the complete tables are provided in the supplementary files (see Code and Data Availability).

5

6 In addition to the general geological principles, the following assumptions govern the tables:

- 7 • **Relata:** are the two geo-objects participating in a binary relation, with their type fixed across all relations in
8 a truth table. For example, for a truth table between a depositional unit A and intrusion unit B, A is the first
9 participant and B is the second participant for all relations in the table, e.g. *A meets B*, *A precedes B*, *B is*
10 *preceded by A*, and *A is aligned with B*. This ensures all possible relation combinations are considered for
11 the pair of objects.
- 12 • **Time:** the framework assumes a geomodel is assessed for consistency at a single point in time. The objects
13 in a geomodel, of course, can develop over different times, but it is their state at a specific time that is
14 evaluated. This impacts the validity of certain geological relations, which might be invalid at a timepoint
15 but valid across timepoints: e.g. two material units cannot share space at a timepoint, but might occupy a
16 common space at different times. There are two main reasons for this choice: (1) practically, most models
17 are developed to reflect a state of geological reality at a single timepoint (typically today); and (2)
18 assessment across time will increase the number of consistencies, and reduce the number of
19 inconsistencies, as many more situations are possible, dramatically increasing complexity and reducing the
20 effectiveness of any consistency-checking approach.
- 21 • **Space:** it is assumed geological objects can be spatially disjoint and possibly very far apart, e.g. on different
22 continents, thus allowing all temporal relations to hold in such cases.
- 23 • **Space-time:** the time assumption implies the objects being assessed are so-called *endurants* or *continuants*,
24 which are fully present at a timepoint, i.e. all parts that can be present at a timepoint are present, such as for
25 a rock, geological unit, or fault surface. This contrasts with so-called *perdurants* or *occurrants*, e.g. space-
26 time worms (4D spatio-temporal objects), processes, or events, which are not fully present at any timepoint,
27 but unfold in time, so are composed of temporal parts that accumulate over time. Then only a temporal part
28 can be fully present at a timepoint, but never the whole worm, process, or event, unless it is instantaneous.
29 *Perdurants/occurrants* are spatially located at the position of their *endurant/continuant* participants, and both

1 participants and their location can change in time. E.g. a ground shaking event - an earthquake - might have
2 discrete early, middle, and late parts, and have the ground and various buildings as participants, but the
3 whole shaking event is not fully present at any timepoint, because it requires all three parts to be complete.
4 The framework assesses only endurants/continuants, and does not check for correct process behavior, for
5 example in simulations.

- 6 • Material sharing: we assume it is physically impossible for macroscopic material objects
7 (endurants/continuants) to share space at a single point in time, unless they share parts, such as one being a
8 part of the other, which restricts the allowable spatial relations between these objects. Consequently, if
9 models are evaluated at a single timepoint, then material sharing is impossible for the material geo-objects
10 outside of part-whole situations, such as a lithology and a geological unit, a formation and a member, or a
11 fabric and its host material unit. We further assume material objects must be volumetric, and can share
12 space with immaterial objects, either volumetric and non-volumetric. E.g. a filled hole shares space with its
13 filling material, and a non-volumetric surface on a material object shares lower-dimensional space with the
14 object. Other non-material objects, such as qualities, e.g. the colour, size, thickness, or shape of an object,
15 also share space with the object carrying them: the grey colour of a rock is not made of material, but
16 occupies the space of its carrying material. It is also tempting to consider tightly intermixed material
17 objects to share space, but this is a physical impossibility – these are simply objects with mixed
18 composition that share neither space nor material at a timepoint. It is also tempting to consider
19 metamorphic units to share space with other units, typically older, but this too is physically impossible at a
20 timepoint, unless one unit is part of the other. In fact, this metamorphic scenario typically consists of the
21 units sharing space, not material, at different times. However, nothing prevents a user or tool from treating
22 metamorphic units as precursor units, e.g. protoliths, during consistency-checking. Although some
23 immaterial objects, such as holes, might share space at a timepoint, e.g. the pore-space of a formation
24 shares space with the pore-space of its member part, these immaterial parthood situations also are excluded.
- 25 • Parthood: although material and immaterial wholes share space with their parts at a timepoint, we exclude
26 such space sharing from the current framework, leaving it to future work. This restricts consistency-
27 checking among certain geo-object pairs, such as between a depositional unit and its material parts, e.g. a
28 group and formation, or the unit and a fabric. However, we do not consider this to be a severe limitation for
29 now: the exclusion does not invalidate the framework nor its use for the very many non-parthood

1 situations; and spatial parthood situations are not currently output by most modeling algorithms. All
2 prevalent algorithms, that we are aware of, will partition objects into non-overlapping spatial regions by
3 design; so if geometric representations from these algorithms have spatially overlapping regions (including
4 for the metamorphic scenarios), then there exists an inconsistency. In future work, we expect parthood to be
5 an additional dimension in our hyperspace, added to the space, time, polarity, and object type dimensions.

- 6 • Model completeness: 3D geo-models are assumed to be complete. Therefore, any two geological objects
7 that touch cannot have objects missing between them, such as an intermediary erosional surface or fault.
8 Without this assumption, the range of consistent scenarios becomes extremely large, with significantly
9 fewer inconsistent scenarios, and the effectiveness of the approach diminishes. Conversely, with this
10 assumption, inconsistent scenarios can signal (but not identify) the absence of spatial intermediaries, which
11 is useful during model-building.

12 **3 Geological Consistency-Checking Tool**

14 The consistency checker workflow is presented in Figure 4. This workflow aims to detect the consistency of 3D geo-
15 models given knowledge inputs of:

- 16 • a 3D geo-model;
- 17 • local knowledge consisting of relative or absolute ages, internal polarities, types of geological objects, and
- 18 • universal knowledge in the form of truth tables reflecting geological norms.

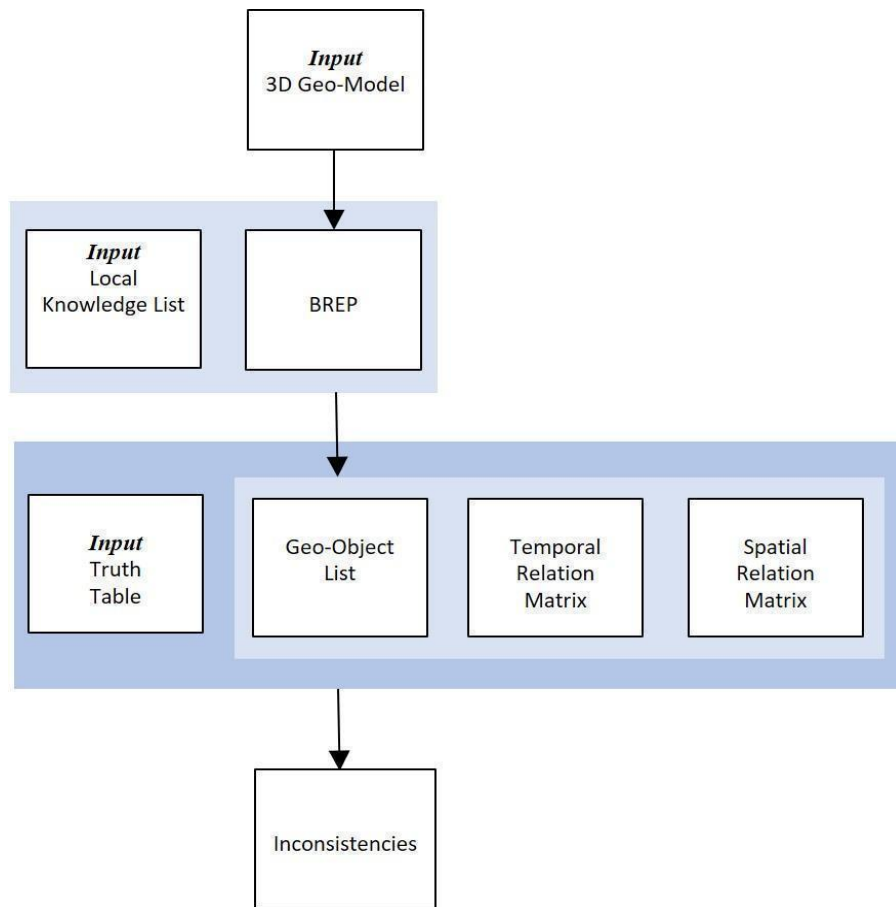
19 After traversal of the 3D geo-model, the consistency checker constructs three intermediary products:

- 20 • a geo-object list, itemizing the geometric objects in the geo-model;
- 21 • a matrix of temporal relations for each pair of geological objects;
- 22 • a matrix of spatial relations for each pair of geological objects;

23 Then, as per Algorithm 1 (see Appendix 1): for each pair of geologic objects, the checker obtains their spatial
24 relation from the spatial relation matrix, their temporal relation from the temporal matrix, and calculates the polarity
25 relation (aligned/opposed) from the objects' internal polarities and temporal relation. These three relations then form
26 an index into a cell within the appropriate truth table to determine consistency. Each geo-object pair is navigated to
27 identify any inconsistent regions, which if present are output as a list of inconsistencies in the geo-model. The tool is
28 written using the Geodes-Solutions spatial toolkit (Botella et al., 2016; Geodes-Solutions; Pellerin 2017), which
29 facilitated spatial navigation and enabled conversion to a volumetric spatial representation where required. It was
30 run on a moderately powerful Windows desktop, typically requiring several minutes to assess a model. Note the tool

1 is written strictly to demonstrate proof-of-concept for the framework and general approach, and is not meant for
2 widespread deployment as it is restricted to an specific, older, version of the toolkit.

3



4

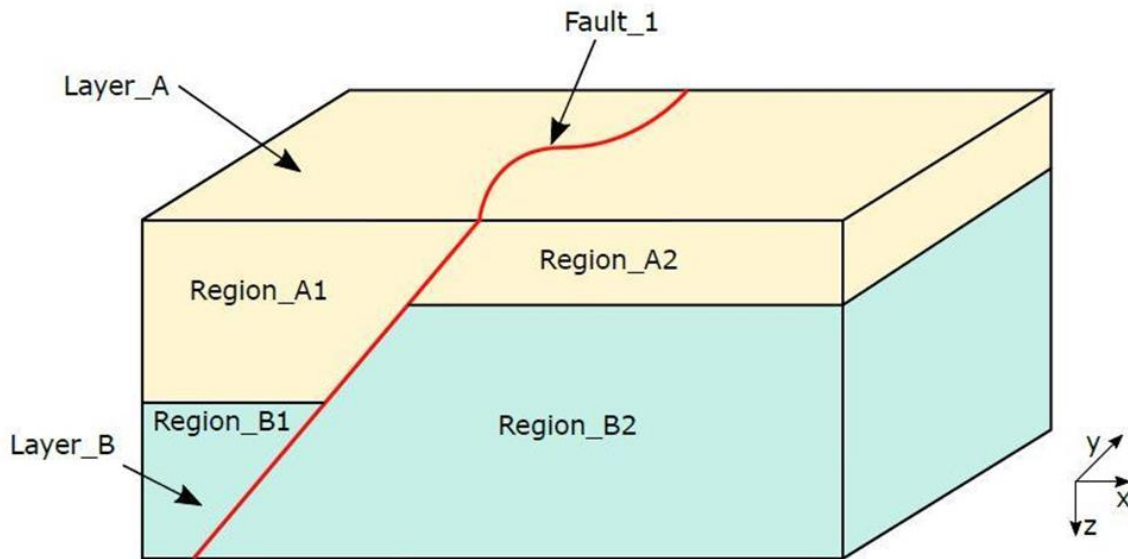
5 **Figure 4.** Consistency checker workflow. BREP - Boundary Representation model (Braid 1975).

6

7 **3.1 Local Knowledge List**

8 Local geological knowledge is specific to each study area and, alongside the 3D geo-model, is a primary input to the
9 consistency checker tool. It is found in a variety of sources external to the 3D geo-model, such as databases, map
10 legends, stratigraphic columns, journal articles and other reports. For the synthetic model shown in Figure 5a, a local
11 knowledge list is developed and illustrated in Figure 5b: the list contains the name of the geological object, its type
12 (from the nine possibilities), global internal polarity and its relative age. For simplicity in the proof-of-concept tool,
13 an object's global polarity is either up, down, or unknown. Also for simplicity in the tool, if a whole geological
14 object is an aggregate of parts, then the local knowledge applies to the whole and is assumed to be the same for
15 every part. For example, in Figure 5a, the local knowledge for units A and B is assumed to also hold for each of

1 their parts A1, A2, B1, B2; separate local knowledge for these parts, if it existed, would not be used. This enables
 2 the spatial, temporal, and polarity to hold between the wholes, which tends to be the resolution at which the input
 3 knowledge is available. However, nothing prevents other implementations of the framework from consistency-
 4 checking the object parts instead of the wholes. Indeed, any simplifications in our tool should not equate to
 5 deficiencies in the framework - they are made only to ease testing, tool-building, and presentation.



6
7
8
9

Figure 5a. example 3D geo-model.

| Geological entity name | Geological entity type | Geological entity polarity | Geological entity age |
|------------------------|---|--------------------------------|-----------------------|
| layer_A | depositional unit / intrusion / extrusion / metamorphic unit / fault / erosion surface / fold volume / linear fabric / planar fabric | up / down / unknown | intermediate |
| layer_B | depositional unit / intrusion / extrusion / metamorphic unit / fault / erosion surface / fold volume / linear fabric / planar fabric | up / down / unknown | oldest |
| fault_1 | depositional unit / intrusion / extrusion / metamorphic unit / fault / erosion surface / fold volume / linear fabric / planar fabric | up / down / unknown | youngest |

10
11
12
13
14
15

Figure 5b. Local knowledge list for the model in Figure 5a.

1 **3.1 Temporal Relation Matrix**

2 Temporal relations are also obtained from external sources, including absolute or relative ages for each geological
 3 object, as well as the kind of duration of the geological event (i.e. interval or instant). This knowledge then
 4 determines the appropriate temporal relation between all pairs of geological objects, organized as a temporal matrix
 5 (Figure 6). The matrix is developed manually for our case studies but could be determined automatically from
 6 databases and other digital sources. The *incomparable* relation is chosen if there exists insufficient knowledge to
 7 determine the temporal relation between a pair of objects.

| | layer_A | layer_B | fault_1 |
|---------|---|---|---|
| layer_A | 6 | 0 / 1 / 2 / 3 / 4 / 5 / 6 / 7 / 8 / 9 / 10 / 11 / 12 / 13 | 0 / 1 / 2 / 3 / 4 / 5 / 6 / 7 / 8 / 9 / 10 / 11 / 12 / 13 |
| layer_B | 0 / 1 / 2 / 3 / 4 / 5 / 6 / 7 / 8 / 9 / 10 / 11 / 12 / 13 | 6 | 0 / 1 / 2 / 3 / 4 / 5 / 6 / 7 / 8 / 9 / 10 / 11 / 12 / 13 |
| fault_1 | 0 / 1 / 2 / 3 / 4 / 5 / 6 / 7 / 8 / 9 / 10 / 11 / 12 / 13 | 0 / 1 / 2 / 3 / 4 / 5 / 6 / 7 / 8 / 9 / 10 / 11 / 12 / 13 | 6 |

Temporal Relations Legend

- 0 = precedes
- 1 = meets
- 2 = overlaps
- 3 = is finished by
- 4 = contains
- 5 = starts
- 6 = equals
- 7 = incomparable to
- 8 = is started by
- 9 = is during
- 10 = finishes
- 11 = is overlapped by
- 12 = is met by
- 13 = is preceded by

8

9 **Figure 6.** Temporal relation matrix for the model in Figure 5a.

10

11 **3.2 Spatial Relation Matrix**

12 Development of the spatial relation matrix within our tool requires transformation of a vectorized 3D geo-model into
 13 a boundary representation (BREP; Banerjee et al., 1981). Such transformation would not be required for
 14 implementations with alternative spatial representations or means of spatial relation determination. The BREP
 15 ensures all geological objects are represented in their full-dimensional form, e.g. a volume initially represented by its
 16 top and bottom surfaces is converted into a mesh of the full exterior limits of the volume, consisting of faces, edges
 17 and vertices. A geo-model then can be traversed by following the geometric decomposition of each object and their
 18 adjacencies. If objects are named and typed (e.g. as in the Geodes-Solutions BREP solution; Botella et al., 2016;
 19 Geodes-Solutions; Pellerin 2017), then such traversal enables building of the spatial relation matrix. Specifically, the
 20 consistency checker tool builds a list containing each geometric object, as well their dimensionality (volume,
 21 surface, or line), type (e.g. depositional unit), and name (e.g. "Layer_A"). The list is traversed in order of
 22 dimensionality, starting with higher-dimensional objects (volumes) and progressing to lower-dimensional objects

1 (surfaces and lines), with spatial relations determined between pairs of objects by inspecting decompositions and
 2 adjacencies. The results are recorded in the spatial relation matrix (Figure 7), which encapsulates the structural and
 3 lithological topology, embedding intuitive geological relations into a computational form; other mechanisms, such
 4 as structural and stratigraphic network graphs, may also be appropriate for representing object relations (Thiele et
 5 al., 2016a, b). For simplicity, a cell in the spatial matrix contains a single value, and the entities being related are the
 6 whole objects, e.g. Layer_A (Figure 5a), and not their parts, e.g. Region_A1 or Region_A2 (Figure 5a). This is
 7 obviously problematic as distinct parts of objects might be spatially related in many ways, e.g. some might touch
 8 and others are disjoint, so the wholes can be related in many ways too, requiring multiple values per cell for each
 9 pair of wholes. For example it is possible Region_A1 has one relation with Region_B1 and a different relation with
 10 Region_B2, thus A would have multiple distinct relations with B. In such cases, the most dominant relation is
 11 selected, which suffices for our case studies. To avoid multi-valued cells, a rigorous approach would utilize object
 12 parts for consistency-checking, rather than the wholes.

| | layer_A | layer_B | fault_1 |
|---------|------------------------------------|------------------------------------|------------------------------------|
| layer_A | 8 | 0 / 1 / 2 / 3 / 4 5 / 6 / 7 / 8 | 0 / 1 / 2 / 3 / 4 5 / 6 / 7 / 8 |
| layer_B | 0 / 1 / 2 / 3 / 4 5 / 6 / 7 / 8 | 8 | 0 / 1 / 2 / 3 / 4 5 / 6 / 7 / 8 |
| fault_1 | 0 / 1 / 2 / 3 / 4 5 / 6 / 7 / 8 | 0 / 1 / 2 / 3 / 4 5 / 6 / 7 / 8 | 8 |

Spatial Relations Legend:

- 0 = disjoint
- 1 = meets / is met
- 2 = intersects
- 3 = overlaps / is overlapped by
- 4 = contains
- 5 = is contained by
- 6 = covers
- 7 = is covered by
- 8 = equals

13

14 **Figure 7.** Spatial relation matrix for the model in Figure 5a.

15

16 **4 Case studies**

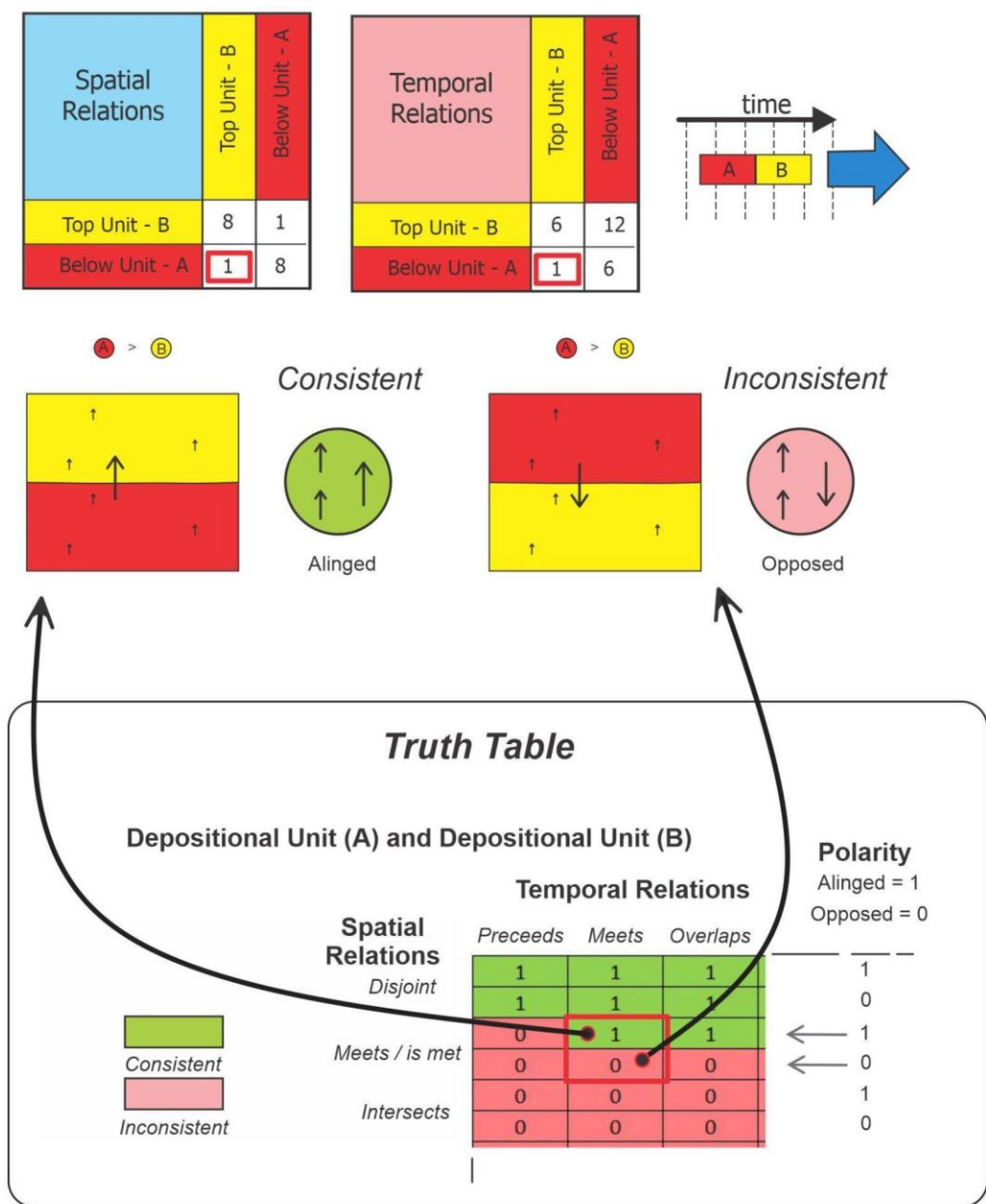
17

18 The consistency checker is tested in four case studies: three synthetic models in which inconsistencies are
 19 introduced, and a real regional geo-model from ongoing project work in Western Canada (Thapa and McMechan,
 20 2019, McMechan et al., 2021). The geo-models are built using a variety of software and underlying approaches
 21 including: Noddy (Jessell, 1981), GOCAD/SKUA (Jayr et al, 2008; Mallet, 2004), GOCAD (Mallet, 1989) and
 22 certain extensions, namely SURFE (Hillier, et al. 2014; de Kemp et al. 2017) and SPARSE (de Kemp et al. 2004).

22

1 **4.1 Implicit Case study**

2 A simple but common modelling error occurs when applying certain implicit algorithms to sparse observations of
3 near parallel, shallow, dipping strata. Then, as depicted in Figure 1, if some older unit data are slightly
4 topographically higher than younger unit data, algorithm bias can result in older units above younger units. To
5 assess such a model, the consistency checker requires alignment of the three polarity vectors, two internal and one
6 temporal: as shown in Figure 8, the CC Truth Table indicates two depositional units that spatially and temporally
7 meet are (1) consistent, if the polarity vectors are aligned, and (2) inconsistent, if they are opposed. Therefore, this
8 model is evaluated as inconsistent, because the temporal polarity vector is opposed to the internal polarity vectors.
9 Note that there could be many reasons for the temporal reversal, but these are not identified by the checker, e.g. it
10 might be algorithmic bias or missing objects, such as absent thrust faults, recumbent folds, or erosional surfaces.

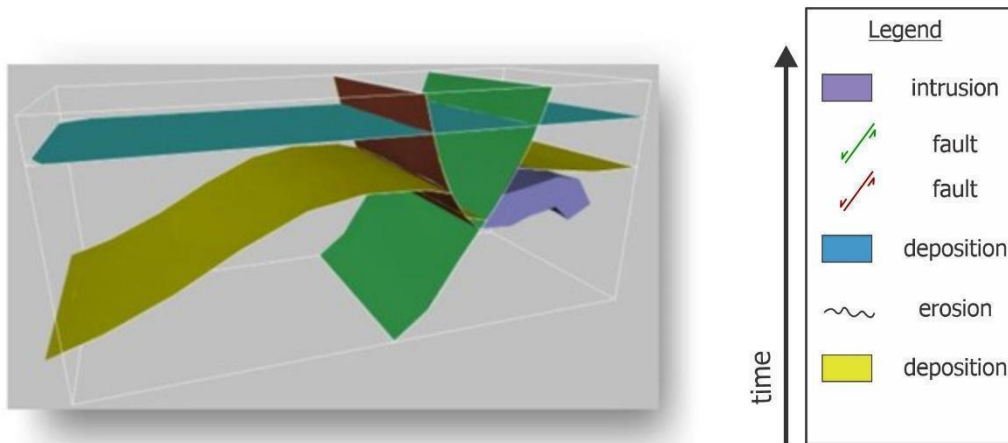


1
2
3
4
5
6
7
8
9
10
11

Figure 8. From the simple model in Figure 1, the internal polarity vectors are aligned with each other, but opposed to the temporal vector. As the units both spatially and temporally *meet*, the CC Truth Table shows this configuration is inconsistent due to the unaligned age vector. Note that a spatial *meets* between these two units is also not allowed if there is a *precedes* temporal relation since there would be a time gap of non-deposition signaling a missing object, in fact a type of erosional surface - a disconformity.

1 **4.2 GOCAD/SKUA Case Study**

2 This synthetic model contains two depositional units, one intrusion, two faults, one fold, and one erosional surface
3 co-located with the top surface of the oldest unit (Figure 9). The model is created with GOCAD/SKUA (Mallet,
4 1989, 2004) using the Structural and Stratigraphic workflow (Jayr et al., 2008); the local knowledge list (Table 4)
5 and temporal matrix (Figure 10) are developed manually. The spatial matrix (Table 5) includes a variety of spatial
6 relations, such as touching geological units, faults cutting geological units, intrusion units protruding into other
7 geological units, as well as disjoint geological objects. As expected, results from the consistency checker indicate
8 the geo-model is geologically consistent. However, if the event timeline is manipulated to generate inconsistencies
9 without altering spatial relations (Figure 11), then an intersection between the second deposited layer (blue) and the
10 first fault (red) is detected, which is inconsistent with the altered event history (Figure 12).



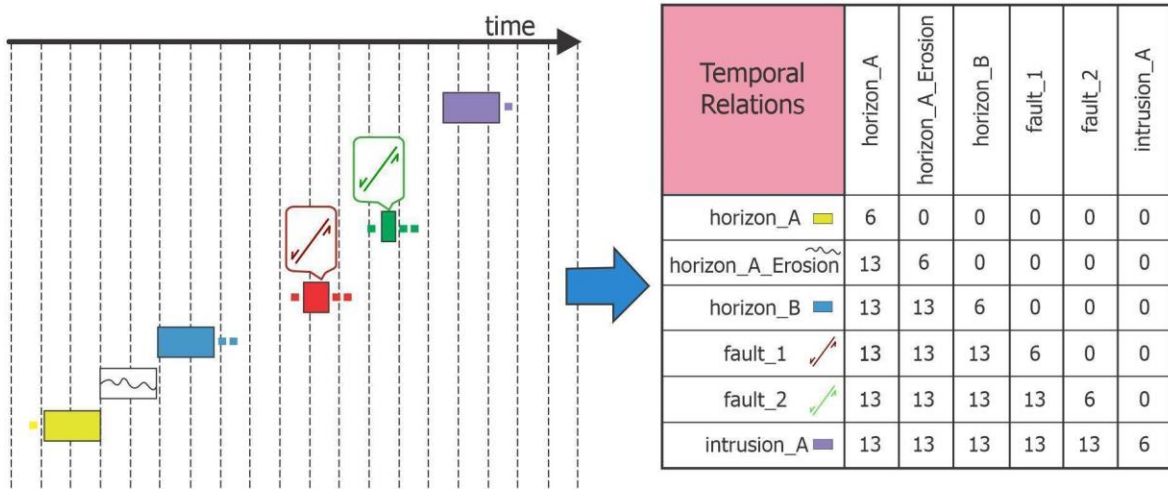
11

12 **Figure 9.** Synthetic geo-model for the GOCAD/SKUA case study: two sedimentary horizons (in yellow and blue),
13 one intrusion (in purple), two faults (in green and red), one fold (in the yellow horizon) and one erosion
14 surface (top of the yellow unit). Horizons define the top of a unit. For simplicity we ignore the folding event
15 that affects pre-erosion sediments.
16

| Name | Entity type | Age | Polarity |
|-------------------|-------------------|----------------------------------|----------|
| Intrusion_A | Intrusion Unit | Youngest | Up |
| Fault_2 | Fault Surface | Younger than F1 | None |
| Fault_1 | Fault Surface | Older than F2 Younger than HB | None |
| Horizon_B | Depositional Unit | Younger than HAE | Up |
| Horizon_A_Erosion | Erosional Surface | Younger than HA | Up |
| Horizon_A | Depositional Unit | Oldest | Up |







1
2
3
4

Table 4. Local knowledge list for the GOCAD/SKUA case study.

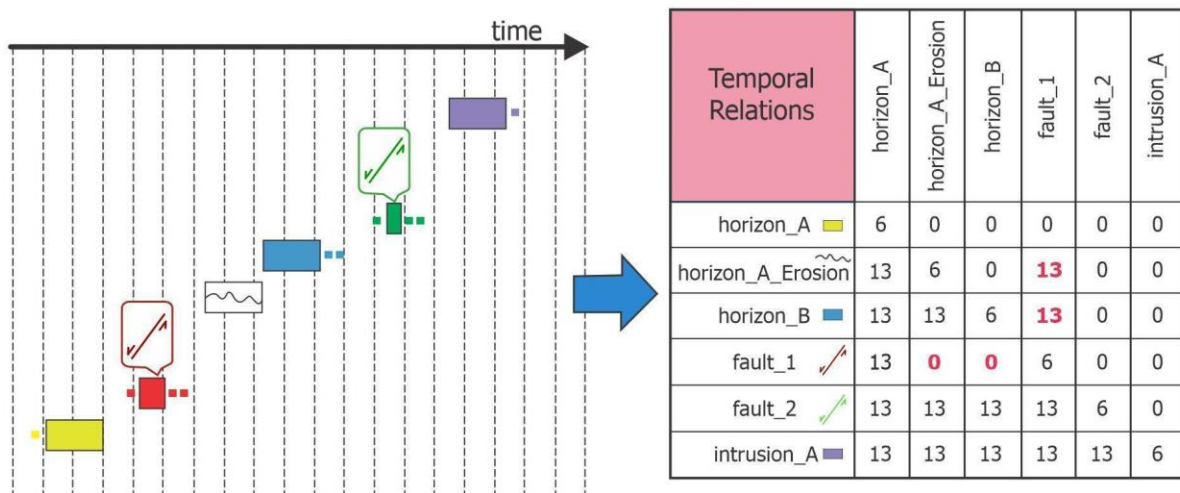


5
6
7

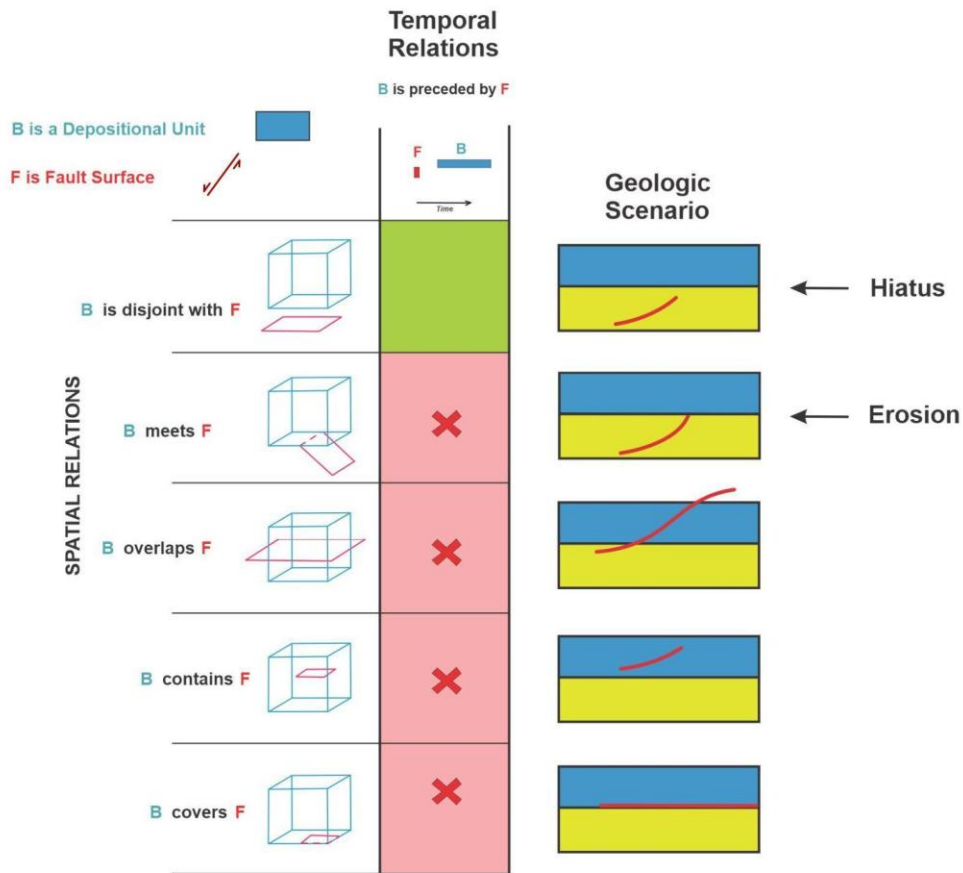
Figure 10. Event history (left) and temporal matrix (right) for the GOCAD/SKUA case study. For temporal relation codes see Figure 6.

| Spatial Relations | horizon_A | horizon_A_Erosion | horizon_B | fault_1 | fault_2 | intrusion_A |
|---|-----------|-------------------|-----------|---------|---------|-------------|
| horizon_A  | 8 | 6 | 1 | 3 | 3 | 1 |
| horizon_A_Erosion  | 6 | 8 | 6 | 2 | 2 | 0 |
| horizon_B  | 1 | 6 | 8 | 3 | 3 | 0 |
| fault_1  | 3 | 2 | 3 | 8 | 1 | 0 |
| fault_2  | 3 | 2 | 3 | 1 | 8 | 6 |
| intrusion_A  | 1 | 0 | 0 | 0 | 6 | 8 |

1
2 **Table 5.** Spatial relation matrix for the GOCAD/SKUA case study. For spatial relation codes see figure 7.



3
4
5 **Figure 11.** Modified event history (left), with red fault earlier in the event history, and temporal matrix (right) for
6 the GOCAD/SKUA case study, with unfeasible temporal relations (in red). For temporal relations codes see
7 Figure 6.



2

3 **Figure 12.** CC Truth Table fragment shows that the geological relation between F (fault_1; earliest fault in red) and
 4 B (Unit B in blue) is inconsistent with the revised geological history in which B *is preceded by* F and B
 5 spatially *overlaps* F. Other inconsistent scenarios (marked 'X') include: B *covers* F, B *contains* F, and B *meets*
 6 F. These are geologically implausible because the early fault (F) was eroded before Unit B was deposited in
 7 the altered history. The only consistent scenario, marked in green, is where F precedes B, allowing for a time
 8 gap in which the fault could be preserved in the underlying host rock. In fact, the inconsistency signals a
 9 missing object, in this case the erosional surface.

10

11

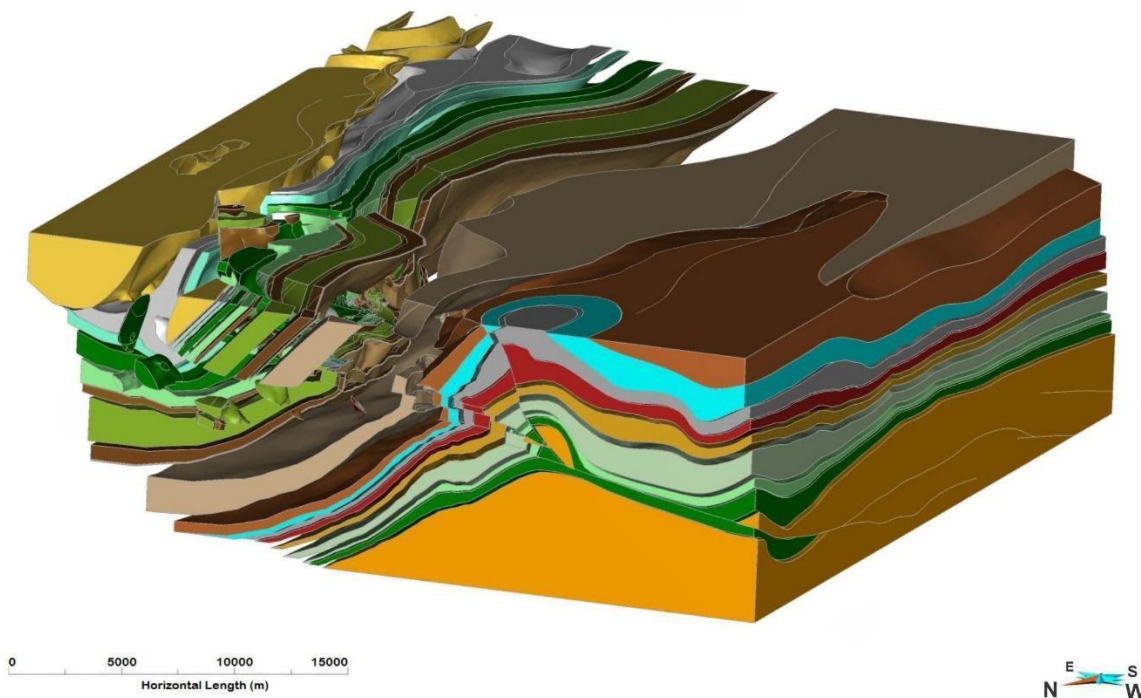
12

13

14

15 **4.3 Western Canada Case Study**

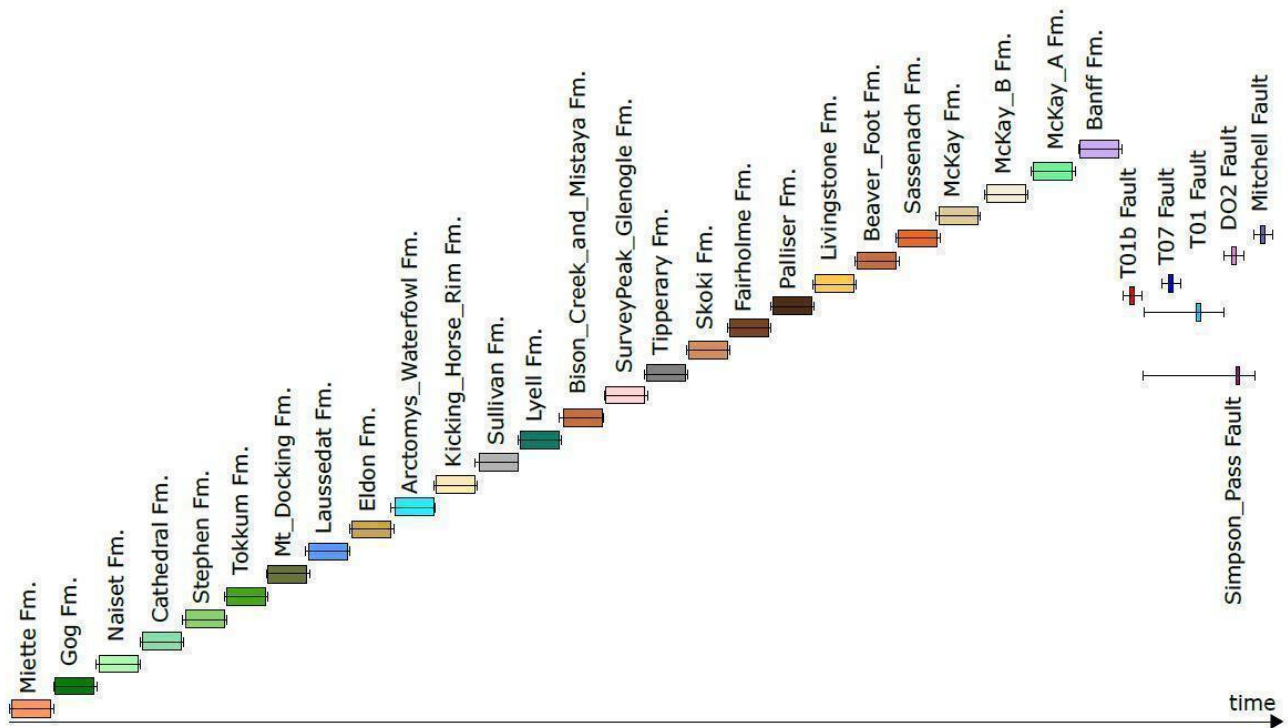
1 The geo-model for this real case study (Figure 13) uses data from the Rocky Mountains of the Western Canadian
2 Cordillera, and is built using the GOCAD/SKUA, SURFE, and SPARSE toolkits (Dutranois, et al. 2010, Hillier et
3 al. 2014, de Kemp et al. 2016). It represents a portion of an east verging fold and thrust belt that has telescoped the
4 Paleozoic and basement meta-sediments of the early North American craton margin, with tectonic deformation
5 having produced in-sequence and out-of-sequence thrusts (McMechan et al., 2021, Morely 1988), as well as later
6 normal faults, with fold-fault and horizon relations that complicate original stratigraphy. The event history (Figure
7 14) is simplified with all the sedimentary units depositing sequentially, and incurring some facies changes across
8 major structures, followed by several episodes of faulting with some overlapping in time. The spatial complexity of
9 the model arises from the multitude of entities, from faults crosscutting other faults and impacting the pre-deposited
10 layers. The resulting geometry is composed of 213 objects within the 25 units, and 6 faults, with each object
11 delimited or separated from the rest of the unit by a fault.



12
13

14 **Figure 13.** Western Canada case study volumetric geo-model: includes 213 objects with 26 geological depositional
15 units and 6 faults. Geology from Thapa and McMechan (2019).

16
17



1
2
3

4 **Figure 14.** Event history for the Western Canada case study: horizontal boxes are relative timelines and bars are
5 possible ranges. Vertical axis could be used for relative spatial properties of objects such as unit thickness,
6 however this information was not available.

7

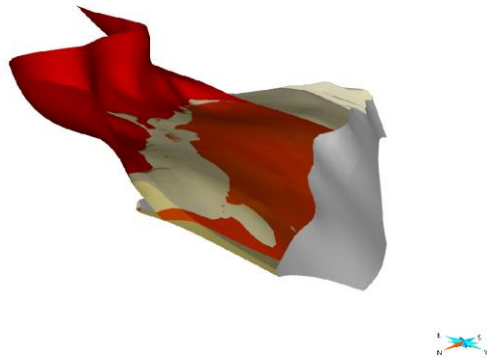
8 After compilation of the local knowledge list and temporal relation matrix from external sources, including maps
9 and reports, and development of the spatial relation matrix (Table 6), the consistency checker detects one
10 inconsistency. The inconsistency (Figure 15) involves the spatial containment of one sedimentary unit
11 (Miette:oldest) by another (Gog:younger), which is impossible given they cannot occupy the same space, being
12 caused by different depositional processes at different times. The consistency checker not only identifies the kind of
13 inconsistency through specification of the truth table cell, but it also pinpoints the location of the problem by
14 identifying the inconsistent volumes, after iteration through all the geo-object pairs. This error would be difficult to
15 detect through visual inspection alone, and if missed could have profound effect on the validity of downstream
16 models such as flow simulations. Subsequent analysis of the inconsistency suggests it is an artifact of the modelling
17 algorithm and its inaccurate interpolation of the data.

18
19

| Spatial Relations | Miette | Gog | Naiset | Cathedral | Tokkumm | Mt_Docking | Laussedat | Eldon | Arctomys_Waterfowl | Kicking_Horse_Rim | Sullivan | Lyell | Bison_Creek_and_Mistaya | SurveyPeak_Glenogle | Tipperary | Skoki | Fairholme | Palliser | Livingstone | Beaver_Foot | Sassenach | McKay | McKay_A | Banff | Kana_Topography | T01b_fault | T07_fault | T01_fault | Simpson Pass_fault | D02_fault | Mitchell_fault |
|----------------------|--------|-----|--------|-----------|---------|------------|-----------|-------|--------------------|-------------------|----------|-------|-------------------------|---------------------|-----------|-------|-----------|----------|-------------|-------------|-----------|-------|---------|-------|-----------------|------------|-----------|-----------|--------------------|-----------|----------------|
| Miette | 8 | 5 | 1 | 1 | 1 | 1 | 1 | 1 | 1 | 1 | 1 | 1 | 1 | 1 | 1 | 1 | 1 | 1 | 1 | 1 | 1 | 1 | 1 | 1 | 3 | 3 | 3 | 3 | 3 | 3 | |
| Gog | 4 | 8 | 1 | 1 | 1 | 1 | 1 | 1 | 1 | 1 | 1 | 1 | 1 | 1 | 1 | 1 | 1 | 1 | 1 | 1 | 1 | 0 | 0 | 0 | 3 | 3 | 0 | 3 | 3 | 3 | |
| Naiset | 1 | 1 | 8 | 1 | 1 | 1 | 1 | 1 | 1 | 1 | 1 | 1 | 1 | 1 | 1 | 1 | 1 | 1 | 1 | 1 | 1 | 0 | 0 | 0 | 3 | 3 | 0 | 3 | 3 | 3 | |
| Cathedral | 1 | 1 | 1 | 8 | 1 | 1 | 1 | 1 | 1 | 1 | 1 | 1 | 1 | 1 | 1 | 1 | 1 | 1 | 1 | 1 | 1 | 0 | 0 | 0 | 3 | 3 | 0 | 3 | 3 | 3 | |
| Tokkumm | 1 | 1 | 1 | 1 | 8 | 1 | 1 | 1 | 1 | 1 | 1 | 1 | 1 | 1 | 1 | 1 | 1 | 1 | 1 | 1 | 1 | 0 | 0 | 0 | 3 | 3 | 0 | 3 | 3 | 3 | |
| Mt_Docking | 1 | 1 | 1 | 1 | 1 | 8 | 1 | 1 | 1 | 1 | 1 | 1 | 1 | 1 | 1 | 1 | 1 | 1 | 1 | 1 | 1 | 0 | 0 | 0 | 3 | 3 | 0 | 3 | 3 | 3 | |
| Laussedat | 1 | 1 | 1 | 1 | 1 | 1 | 8 | 1 | 1 | 1 | 1 | 1 | 1 | 1 | 1 | 1 | 1 | 1 | 1 | 1 | 1 | 0 | 0 | 0 | 3 | 3 | 0 | 3 | 3 | 3 | |
| Eldon | 1 | 1 | 1 | 1 | 1 | 1 | 1 | 8 | 1 | 1 | 1 | 1 | 1 | 1 | 1 | 1 | 1 | 1 | 1 | 1 | 1 | 0 | 0 | 0 | 3 | 3 | 0 | 3 | 3 | 3 | |
| Arctomys_Waterfowl | 1 | 1 | 1 | 1 | 1 | 1 | 1 | 1 | 8 | 1 | 1 | 1 | 1 | 1 | 1 | 1 | 1 | 1 | 1 | 1 | 1 | 0 | 0 | 0 | 3 | 3 | 0 | 3 | 3 | 3 | |
| Kicking_Horse_Rim | 1 | 1 | 1 | 1 | 1 | 1 | 1 | 1 | 1 | 8 | 1 | 1 | 1 | 1 | 1 | 1 | 1 | 1 | 1 | 1 | 1 | 0 | 0 | 0 | 3 | 3 | 3 | 3 | 3 | 3 | |
| Sullivan | 1 | 1 | 1 | 1 | 1 | 1 | 1 | 1 | 1 | 1 | 8 | 1 | 1 | 1 | 1 | 1 | 1 | 1 | 1 | 1 | 1 | 0 | 0 | 0 | 3 | 3 | 3 | 3 | 3 | 3 | |
| Lyell | 1 | 1 | 1 | 1 | 1 | 1 | 1 | 1 | 1 | 1 | 1 | 8 | 1 | 1 | 1 | 1 | 1 | 1 | 1 | 1 | 1 | 0 | 0 | 1 | 3 | 3 | 3 | 3 | 3 | 3 | |
| Bison_Creek_Mistaya | 1 | 1 | 1 | 1 | 1 | 1 | 1 | 1 | 1 | 1 | 1 | 1 | 8 | 1 | 1 | 1 | 1 | 1 | 1 | 1 | 1 | 0 | 0 | 1 | 3 | 3 | 3 | 3 | 3 | 3 | |
| Survey_Peak_Glenogle | 1 | 1 | 1 | 1 | 1 | 1 | 1 | 1 | 1 | 1 | 1 | 1 | 1 | 8 | 1 | 1 | 1 | 1 | 1 | 1 | 1 | 0 | 1 | 3 | 3 | 3 | 3 | 3 | 3 | 3 | |
| Tipperary | 1 | 1 | 1 | 1 | 1 | 1 | 1 | 1 | 1 | 1 | 1 | 1 | 1 | 1 | 8 | 1 | 1 | 1 | 1 | 1 | 1 | 1 | 1 | 1 | 3 | 3 | 3 | 3 | 3 | 3 | |
| Skoki | 0 | 1 | 1 | 1 | 1 | 1 | 1 | 1 | 1 | 1 | 1 | 1 | 1 | 1 | 1 | 8 | 1 | 1 | 1 | 1 | 1 | 1 | 1 | 3 | 3 | 3 | 3 | 3 | 3 | 3 | |
| Fairholme | 0 | 1 | 1 | 1 | 1 | 1 | 1 | 1 | 1 | 1 | 1 | 1 | 1 | 1 | 1 | 1 | 8 | 1 | 1 | 1 | 1 | 1 | 1 | 3 | 3 | 3 | 3 | 3 | 3 | 3 | |
| Palliser | 0 | 1 | 1 | 1 | 1 | 1 | 1 | 1 | 1 | 1 | 1 | 1 | 1 | 1 | 1 | 1 | 1 | 8 | 1 | 1 | 1 | 1 | 1 | 3 | 3 | 3 | 3 | 3 | 3 | 0 | |
| Livingstone | 0 | 1 | 1 | 1 | 1 | 1 | 1 | 1 | 1 | 1 | 1 | 1 | 1 | 1 | 1 | 1 | 1 | 1 | 8 | 1 | 1 | 1 | 1 | 3 | 3 | 3 | 3 | 3 | 3 | 0 | |
| Beaver_Foot | 0 | 1 | 1 | 1 | 1 | 1 | 1 | 1 | 1 | 1 | 1 | 1 | 1 | 1 | 1 | 1 | 1 | 1 | 1 | 8 | 1 | 1 | 1 | 3 | 3 | 3 | 3 | 3 | 3 | 0 | |
| Sassenach | 0 | 1 | 1 | 1 | 1 | 1 | 1 | 1 | 1 | 1 | 1 | 1 | 1 | 1 | 1 | 1 | 1 | 1 | 1 | 1 | 8 | 1 | 1 | 3 | 3 | 3 | 3 | 3 | 3 | 0 | |
| McKay | 0 | 0 | 0 | 0 | 1 | 0 | 0 | 0 | 0 | 0 | 0 | 0 | 0 | 0 | 1 | 1 | 1 | 1 | 1 | 1 | 1 | 8 | 1 | 3 | 3 | 3 | 3 | 3 | 3 | 0 | |
| McKay_A | 0 | 0 | 0 | 0 | 0 | 0 | 0 | 0 | 0 | 0 | 0 | 0 | 0 | 0 | 1 | 1 | 1 | 1 | 1 | 1 | 1 | 1 | 8 | 1 | 3 | 0 | 3 | 3 | 0 | 3 | 0 |
| Banff | 0 | 0 | 0 | 0 | 0 | 0 | 0 | 0 | 0 | 0 | 0 | 0 | 1 | 1 | 1 | 1 | 1 | 1 | 1 | 1 | 1 | 1 | 1 | 8 | 3 | 3 | 3 | 3 | 3 | 0 | |
| Kana_Topography | 3 | 3 | 3 | 3 | 3 | 3 | 3 | 3 | 3 | 3 | 3 | 3 | 3 | 3 | 3 | 3 | 3 | 3 | 3 | 3 | 3 | 3 | 3 | 8 | 2 | 2 | 2 | 2 | 2 | 2 | |
| T01b_fault | 3 | 3 | 3 | 3 | 3 | 3 | 3 | 3 | 3 | 3 | 3 | 3 | 3 | 3 | 3 | 3 | 3 | 3 | 3 | 3 | 3 | 3 | 0 | 3 | 2 | 8 | 0 | 0 | 1 | 0 | 0 |
| T07_fault | 3 | 3 | 3 | 3 | 3 | 3 | 3 | 3 | 3 | 3 | 3 | 3 | 3 | 3 | 3 | 3 | 3 | 3 | 3 | 3 | 3 | 3 | 3 | 2 | 0 | 8 | 0 | 1 | 1 | 1 | |
| T01_fault | 0 | 0 | 0 | 0 | 0 | 0 | 0 | 0 | 0 | 3 | 3 | 3 | 3 | 3 | 3 | 3 | 3 | 3 | 3 | 3 | 3 | 3 | 3 | 2 | 0 | 0 | 8 | 0 | 1 | 0 | |
| Simpson Pass_fault | 3 | 3 | 3 | 3 | 3 | 3 | 3 | 3 | 3 | 3 | 3 | 3 | 3 | 3 | 3 | 3 | 3 | 3 | 3 | 3 | 3 | 3 | 0 | 3 | 2 | 1 | 1 | 0 | 8 | 0 | 0 |
| D02_fault | 3 | 3 | 3 | 3 | 3 | 3 | 3 | 3 | 3 | 3 | 3 | 3 | 3 | 3 | 3 | 3 | 3 | 3 | 3 | 3 | 3 | 3 | 3 | 2 | 0 | 1 | 1 | 0 | 8 | 1 | 1 |
| Mitchell_fault | 3 | 3 | 3 | 3 | 3 | 3 | 3 | 3 | 3 | 3 | 3 | 3 | 3 | 3 | 3 | 3 | 3 | 3 | 3 | 3 | 3 | 3 | 3 | 2 | 0 | 1 | 0 | 0 | 1 | 8 | 8 |

Spatial Relations Legend: 0 = disjoint 3 = overlaps, is overlaped by 6 = covers
1 = meets, is met by 4 = contains 7 = is covered by
2 = intersects 5 = is contained by 8 = equals

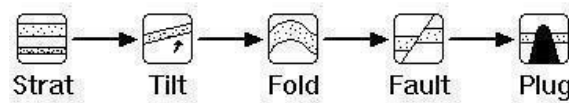
1
2 **Table 6.** Spatial relation matrix for the Western Canada case study; inconsistent containment relations are in red as
3 *contains* (4) and *is contained by* (5). Depositional unit - fault relations are either *disjoint* (0) or *overlap* (3). Fault
4 and topography relations labeled as *intersects* (2) since the model extends above topography, similarly volumetric
5 units are in *overlap* (3) relation with the topographic surface. Most Unit - Unit relations are spatial *meets* (1) or
6 *disjoint* (0).



7
8 **Figure 15.** Inconsistent spatial containment between the Gog (red) and Miette (yellow) units in the Western Canada
9 case study. The Miette is an older unit preceding deposition of Gog material, so there should not be a 'Miette
10 *contains* Gog' or 'Gog is contained by Miette' spatial relation.

1
2 **4.4 Noddy Case Study**

3 The synthetic geo-model for this case study is generated using Noddy, which is a 3D rule-based modelling tool
4 (Jessell, 1981) that applies an input list of geological events, or event schema (Perrin et al. 2013), to a volume of
5 interest from which a spatial topology can be generated between objects in the volume. The event history for this
6 case study is quite simple, including 5 major events, deposition, tilting, folding, faulting, and intrusion (Figure 16),
7 from which the local knowledge list and temporal matrix are derived. The resulting geo-model (Figure 17) has an
8 initial depositional sequence involving 6 depositional units (represented by their top horizons), an early tilting event
9 followed by folding and normal faulting, and an intrusive body subsequently injected into all previous geological
10 objects, with the fault cutting all the horizons but not the intrusion body. Navigation of the BREP representation of
11 the geo-model yields a rich temporal matrix (Table 7) and spatial matrix (Table 8a).



13 **Figure 16.** Event history for the Noddy case study: the Stratigraphic event is the deposition of 6 geological units in
14 sequence.

15

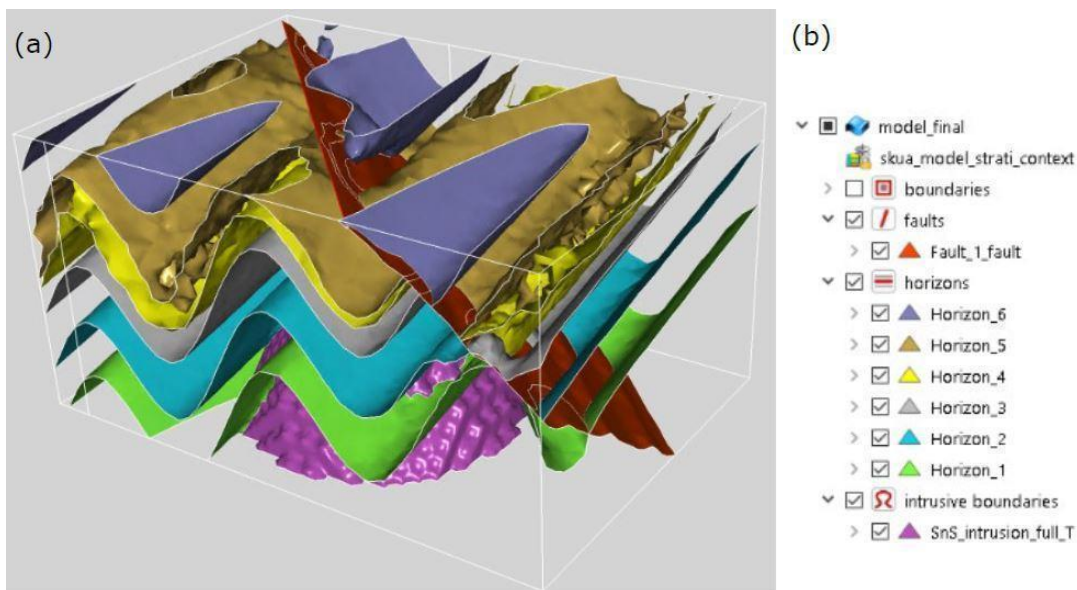


Figure 17. 3D geo-model for the Noddy case study.

| TIME | Horizon_1 | Horizon_2 | Horizon_3 | Horizon_4 | Horizon_5 | Horizon_6 | Above Horizon 6 | Fault | Intrusion |
|-----------------|-----------|-----------|-----------|-----------|-----------|-----------|-----------------|-------|-----------|
| Horizon_1 | 6 | 0 | 0 | 0 | 0 | 0 | 0 | 0 | 0 |
| Horizon_2 | 13 | 6 | 0 | 0 | 0 | 0 | 0 | 0 | 0 |
| Horizon_3 | 13 | 13 | 6 | 0 | 0 | 0 | 0 | 0 | 0 |
| Horizon_4 | 13 | 13 | 13 | 6 | 0 | 0 | 0 | 0 | 0 |
| Horizon_5 | 13 | 13 | 13 | 13 | 6 | 0 | 0 | 0 | 0 |
| Horizon_6 | 13 | 13 | 13 | 13 | 13 | 6 | 0 | 0 | 0 |
| Above Horizon 6 | 13 | 13 | 13 | 13 | 13 | 13 | 6 | 0 | 0 |
| Fault | 13 | 13 | 13 | 13 | 13 | 13 | 13 | 6 | 0 |
| Intrusion | 13 | 13 | 13 | 13 | 13 | 13 | 13 | 13 | 6 |

1

2

Table 7. Temporal relations matrix for the Noddy case study. Temporal codes used here: 0 = precedes, 6 = equals, 13 = preceded by.

3

4

5

As a knowledge-based geo-modelling tool, Noddy will always produce a consistent model. However, export to

6

GOCAD/SKUA via the DXF file format results in a different spatial relation matrix, one that introduces several

7

geologically consistent but nevertheless suspect spatial relations: every unit spatially *meets* (i.e. touches) every other

8

unit (Table 8b). Although not impossible, this is somewhat suspicious, given it contradicts the original Noddy

9

model. As the resolution of the Noddy model is quite low, it seems likely that mesh extents might have been mis-

10

calculated during export to GOCAD/SKUA.

11

a)

| SPACE | Horizon_1 | Horizon_2 | Horizon_3 | Horizon_4 | Horizon_5 | Horizon_6 | Above Horizon 6 | Fault | Intrusion |
|-----------------|-----------|-----------|-----------|-----------|-----------|-----------|-----------------|-------|-----------|
| Horizon_1 | 8 | 1 | 0 | 0 | 0 | 0 | 0 | 2 | 2 |
| Horizon_2 | 1 | 8 | 1 | 0 | 0 | 0 | 0 | 2 | 2 |
| Horizon_3 | 0 | 1 | 8 | 1 | 0 | 0 | 0 | 2 | 2 |
| Horizon_4 | 0 | 0 | 1 | 8 | 1 | 0 | 0 | 2 | 2 |
| Horizon_5 | 0 | 0 | 0 | 1 | 8 | 1 | 0 | 2 | 2 |
| Horizon_6 | 0 | 0 | 0 | 0 | 1 | 8 | 1 | 2 | 2 |
| Above Horizon 6 | 0 | 0 | 0 | 0 | 0 | 1 | 8 | 2 | 2 |
| Fault | 2 | 2 | 2 | 2 | 2 | 2 | 2 | 8 | 0 |
| Intrusion | 2 | 2 | 2 | 2 | 2 | 2 | 2 | 0 | 8 |

b)

| SPACE | Horizon_1 | Horizon_2 | Horizon_3 | Horizon_4 | Horizon_5 | Horizon_6 | Above Horizon 6 | Fault | Intrusion |
|-----------------|-----------|-----------|-----------|-----------|-----------|-----------|-----------------|-------|-----------|
| Horizon_1 | 8 | 1 | 1 | 1 | 1 | 1 | 1 | 2 | 2 |
| Horizon_2 | 1 | 8 | 1 | 1 | 1 | 1 | 1 | 2 | 2 |
| Horizon_3 | 1 | 1 | 8 | 1 | 1 | 1 | 1 | 2 | 2 |
| Horizon_4 | 1 | 1 | 1 | 8 | 1 | 1 | 1 | 2 | 2 |
| Horizon_5 | 1 | 1 | 1 | 1 | 8 | 1 | 1 | 2 | 2 |
| Horizon_6 | 1 | 1 | 1 | 1 | 1 | 8 | 1 | 2 | 2 |
| Above Horizon 6 | 1 | 1 | 1 | 1 | 1 | 1 | 8 | 2 | 2 |
| Fault | 2 | 2 | 2 | 2 | 2 | 2 | 2 | 8 | 0 |
| Intrusion | 2 | 2 | 2 | 2 | 2 | 2 | 2 | 0 | 8 |

1

2 **Table 8.** Spatial relations matrix for Noddy case study, including (a) original model, and (b) after export via DXF to
 3 GOCAD/SKUA. Note the replacement of many *is disjoint with* relations (**0**) in (a), with *meets / is met by* (**1**) in
 4 (b). This export operation essentially results in elimination of unit-unit *disjoint* spatial relations that will, upon
 5 re-importing into other applications, drastically distort the actual geometric relations.

1
2
3
4
5
6
7
8
9
10
11
12
13
14
15
16
17
18
19
20
21
22
23
24
25
26
27
28
29
30

5 Discussion

The consistency-checking framework and tool presented in this article are a first step toward the automated assessment of geological consistency in 3D geological models. The approach yields promising results in the four case studies: given minimal knowledge typically accompanying a 3D model, it detects geological inconsistencies that contravene universal geological norms captured by the truth tables. However, there is much room for improvement in determining the consistency of complex situations: the checker assesses the validity of a single geological relation in isolation, but as evident from the Noddy case study (Table 8b), a collection of relations can be inconsistent even if each relation is consistent. The consistency of such relation combinations remains a future task.

To help differentiate the various model realizations, another future consideration is the development of consistency metrics for quantitative assessment of the overall quality of a 3D geo-model. These might include a cumulative consistency score to gauge the overall effect of inconsistencies on the model, as well as perhaps targeted consistency scores for specific geo-feature relations. The latter would be particularly useful to differentiate (1) models with few inconsistencies but deep impact on internal model architecture, from (2) models with many inconsistencies but low impact on internal architecture.

Several aspects of the consistency-checking tool could be improved:

- API: development of a simple API (Application Programming Interface) to the truth tables, to enable consistency-checking from a variety of software environments, including possibly those with streamlined spatial navigation mechanisms not necessarily requiring conversion to BREP.
- Enhanced Output: from the current application or prospective API, to enhance both formatting and content, such as encoding conflicting objects using knowledge graphs or spatial standards, to facilitate visualization and understanding.

Aspects of the framework also could be improved:

- Polarity: more automated tools could be incorporated to determine polarities. The internal polarity of an object is rarely available in local knowledge, though potentially can be calculated from the modelling algorithm, e.g. as part of the scalar field gradient direction in implicit modelling, or calculation from the local normals of a

1 triangulated surface. A further refinement might use local internal polarity vectors to determine polarity
2 relations, rather than global vectors. Supplementation from other data and methods would also be beneficial,
3 e.g. from various point observations, depositional top orientations and paleoflow trends, erosional surfaces,
4 cooling surface directions (of an intrusion or extrusion), the regional or contact metamorphic gradient for a
5 metamorphic unit, or directional tectonic information such as fold vergence and principal strain gradients
6 (Fossen, 2016; Alsop, 1999; Finkl, 1984). Fold vergence could be particularly useful: if it contradicts the
7 metamorphic polarity of a large orogenic terrane unit (90-180 degrees) then the situation could be inconsistent.
8 Generally, folds will verge away from the core or deeper axis of an orogen and these directions might be useful
9 in discerning juxtaposition with other objects with polarity.

- 10 • Alternate representations: it would be interesting to implement the framework on lower-dimensional
11 representations of geo-objects, e.g. maps and cross-sections.
- 12 • Geo-object types: consistency-checking also could be improved conceptually by expanding the list of
13 geological objects to include fault types (e.g. normal, reverse, strike slip) and fault domains (e.g. upper-
14 crust/thin-skin, deep-crust/ductile); or adding kinematic directions as another parameter in the truth tables.
15 These would enable, for example, comparison of macro properties such as nature of the deformation system
16 with the observed local kinematic conditions, e.g. thrusting or normal fault displacements.
- 17 • Parthood: as most 3D modeling algorithms and tools typically do not generate solid volumes in which one is
18 fully contained or covered by the other, we have set these relations as invalid for this work, knowing their
19 presence likely indicates a modeling problem and hence an inconsistency. However, algorithms will no doubt
20 mature, so future work should amend the truth tables to reflect the potential validity of such cases. This might
21 include further extended parameters, such as for parthood to indicate if a geological object is validly part of
22 another, e.g. a formation part of a group, or a fabric part of its host rock.

23
24 More generally, broadening the underlying notion of reasonableness, which thus far is roughly equated with
25 consistency, would yield further theoretical gains. An important assumption in the existing approach is the
26 correctness of input geological knowledge. As such knowledge typically reflects the understanding of domain
27 experts, inconsistent models often differ from the expectations of these experts (van Giffen et al., 2022; McKay and
28 Harris, 2016; Burch, 2003). However, the correctness of input knowledge is a dangerous assumption, as it is more
29 likely that input knowledge is incomplete and has gaps, biasing expert expectations. It is necessary then to broaden

1 notions of geological reasonableness beyond the binary categories of consistent and inconsistent. Indeed, if we
 2 consider input knowledge might be grossly good (e.g. true) or bad (e.g. false), and models consistent or inconsistent
 3 with input knowledge, then four kinds of reasonableness emerge, as per Table 9: reasonable, unreasonable,
 4 reasonably bad, and unreasonably bad. Reasonable models, generally preferred, are consistent with good input
 5 knowledge and data constraints. Unreasonable models have geological relations inconsistent with good input
 6 knowledge. Reasonably bad models have geological relations that fit with the input knowledge, but this knowledge
 7 is wrong, or incomplete, so the model is variously questionable. Unreasonably bad models have input knowledge
 8 that may be wrong, and the model is also inconsistent, because of algorithm bias, scale/resolution, constraint data
 9 configuration or other processing errors. Inconsistent models thus signal a need to adjust the algorithm or investigate
 10 the input data and knowledge. Note, however, all models might be useful (Gleeson et al, 2021), as any geo-model
 11 from bad knowledge might be preferred to no models, or models with no input knowledge; and an inconsistent
 12 model from good knowledge, that is unreasonable, might be preferable to the alternatives, especially in parts where
 13 it is actually consistent.

14
15

| | | Model Consistency | |
|-----------------------|--|--------------------------|-------------------|
| | | Inconsistent | Consistent |
| Good Knowledge | | Unreasonable | Reasonable |
| Bad Knowledge | | Unreasonably Bad | Reasonably Bad |

16

17 **Table 9.** Types of 3D geo-model consistency.

18

19 It is also noteworthy, and sobering, that an ideal model - i.e. one close to reality and matching input data - could
 20 arise from any of the four categories, simply because the combination of input knowledge, data, and computational
 21 processes just happens to produce the best result. Consistency-checking thus provides only some insight as to
 22 whether an ideal model is achieved, as one would hope an ideal model should be consistent more often than not. For
 23 example this should be the case when comparing a suite of models and their flow characteristics, with ‘reasonable’

1 models matching the real world historical production curves (Melnikova et al., 2012). Mounting evidence suggests
2 even a minimum of geological knowledge and improved consistency with this knowledge can improve the utility of
3 models (Giraud et al., 2020, Bond et al. 2015). Enhancing our ability to embed this knowledge into 3D workflows
4 will be an ongoing and important task to increase potential for developing more reasonable geological models
5 (Maxelon et al. 2009).

6
7 Finally, application of the framework to case studies at various scales, using different tools and algorithms, would
8 provide further insight into its utility for: exploring different levels of geological and model complexity (Pellerin et
9 al., 2015); comparing high-resolution to generalized regional models; testing more speculative models; for
10 correlation of jurisdictional bordered models (e.g. comparing number and variety of entities, and consistency with
11 each other); and finally for assessing the range of possible 3D geological models created from probabilistic and
12 future generative AI methods.

13

14 **6 Conclusions**

15 Due to the increasing complexity of current geo-modelling algorithms, leading to a plethora of models of variable
16 quality, there is a clear need for a quick and easy-to-use approach to check the geological consistency of a model.

17 The consistency checker framework and proof-of-concept tool developed in this paper successfully verify geo-
18 models in four case studies, confirming consistencies and finding inconsistencies. Inputs include knowledge
19 typically available with any geological model, namely, the spatial-temporal-polarity relations between pairs of
20 geological objects. A specific combination of these inputs serves as an index into a CC Truth Table to document a
21 possible geological situation that is either consistent or inconsistent with established geological principles.

22 Altogether, this work represents a first step toward the real-time consistency-checking of geo-models; therefore, it is
23 also potentially a first step toward interim consistency-checking during model-building, to help increase knowledge
24 constraints in geo-modelling algorithms.

25
26
27
28
29
30
31
32
33
34
35

1
2 **Appendix 1**

3
4 **Algorithm 1: Consistency-checking**

5
6 **Require:** *Mspatial* spatial relationship matrix, *Mtemporal* temporal relationship matrix, *LNaturePolarity* nature and
7 polarity matrix of entities, *TruthTable* 'Truth Tables' for each pair of geological entities, *LGeologicalEntities* list
8 of all geological entities detected in the 3D model.

9 **Initialize (empty):** *Linconsistencies* list of inconsistencies detected inside the given 3D geological model

10 **for** each *GeolEntity* in *LGeologicalEntities* **do**

11 **for** each *GeolEntity* in the remaining rows in *LGeologicalEntities* **do**

12 extract the name, nature and polarity in each geological entity from *LNaturePolarity*

13 given both geological entities, find the corresponding truth table *TruthTable*

14 deduce the polarity relation from both geological entities: aligned, opposed, unknown

15 extract the spatial relationship for the pair of geological entities from *Mspatial*

16 transform the spatial relationship into a row in the truth table

17 extract the temporal relationship for the pair of geological entities from *Mtemporal*

18 transform the temporal relationship into a column in the truth table

19 **if** the statement found in the corresponding truth table is 'inconsistent' **then**

20 **for** each part in each *GeolEntity* **do**

21 **for** each part in each *GeolEntity* **do**

22 extract the name, nature and polarity of each geological entity inside *LNaturePolarity*

23 given both geological entities, find the corresponding truth table *TruthTable*

24 deduce the polarity relation from both geological entities: aligned, opposed, unknown

25 extract the spatial relationship for the pair of geological entities from *Mspatial*

26 transform the spatial relationship into a row in the truth table

27 extract the temporal relationship for the pair of geological entities from *Mtemporal*

28 transform the temporal relationship into a column in the truth table

29 **if** the statement found in the corresponding truth table is 'inconsistent' **then**

30 **for** each part in each part of *GeolEntity* **do**

31 **for** each part in each part of *GeolEntity* **do**

32 etc...

33 **end for**

34 **end for**

35 **end if**

36 **end for**

37 **end for**

38 **end if**

39 add the statement found in the corresponding truth table to *Linconsistencies*

40 **end for**

41 **end for**

42 **return** *Linconsistencies*

43

44

45

46

47

48

49

50

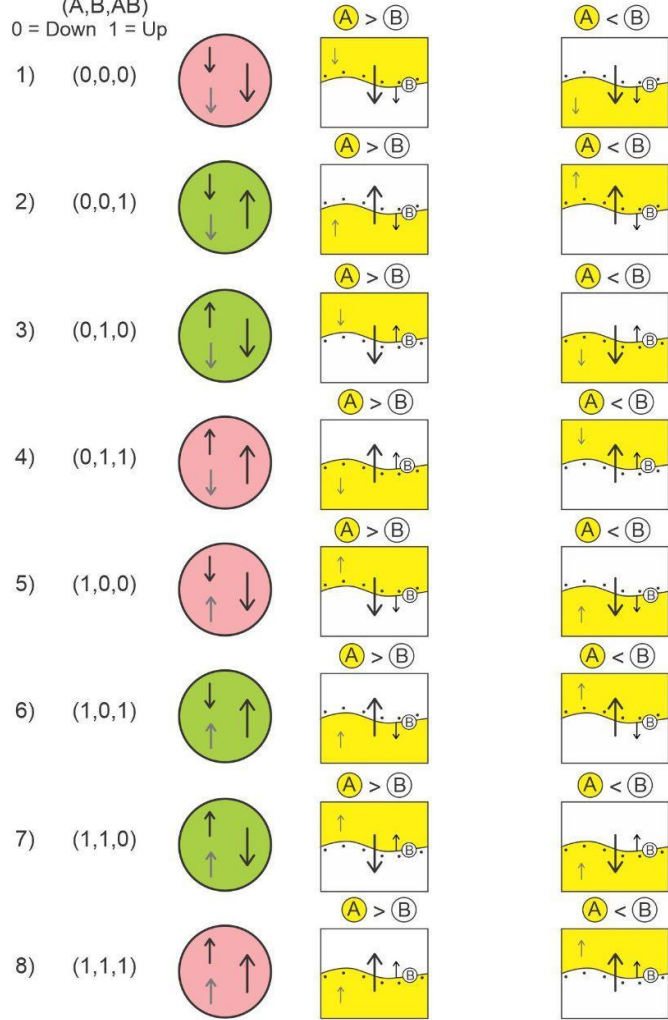
1 **Appendix 2** Detailed Deposition- Erosion consistency checking examples.

Depositional Unit (A) - Erosional Surface (B)

Spatial Covers

Relative Polarity Directions

(A,B,AB)
0 = Down 1 = Up



Legend

> Older than
< Younger than

Consistent
Age polarity (older to younger)
Internal polarity
Opposed

Inconsistent
Age polarity (older to younger)
Internal polarity
Aligned

1 Polarity configuration examples for geological relations between **Depositional Unit (A) - Erosional Surface (B)**.
2 Spatial *covers* and temporal *precedes* are used. Note that Case 1) and 8) are equivalent as well as Case 4) and 5),
3 and these are inconsistent. Case 2) and 7) are equivalent as well as Case 3) and 6), all are consistent. Case 7 (A < B)
4 is perhaps an end member consistent case, for example a Karst cavern ceiling being sealed (covered) with sediment
5 from the bottom to seal the roof.

6 **Code and Data Availability**

7 Consistency-inconsistency matrices, called CC Truth Tables, used for determining validity of geological spatial-
8 temporal relations; <https://doi.org/10.5281/zenodo.13948382> last access: 17 October 2024, (de Kemp, 2024).

10 **Video Supplement**

11 There are currently no video files (mp4) related to this article.

12 **Author contributions**

13 Conceptualization by MP, EdK, BB and MH; MP developed the system; MP, EdK, BB and MH all contributed to
14 the case studies development and the writing of the paper.

15 **Competing interests**

16 The author declares that there is no conflict of interest.

17 **Special Issue Statement:** This contribution is part of the Loop stochastic geological modelling platform –
18 development and applications, edited by Laurent Ailleres
19 (https://gmd.copernicus.org/articles/special_issue1142.html, last access: 6 April 2024).

20 **Acknowledgements**

21 Generous support for this research was provided from the Canada3D project (C3D), through the Open Geoscience
22 Initiative of Natural Resources Canada (<https://canada3d.geosciences.ca/>, last access: 6 April 2024). Support from
23 the LOOP project (<https://loop3d.github.io/>, last access: 6 April 2024), Australian Research Council (ARC);
24 (Enabling Stochastic 3D Geological Modelling, LP170100985), in collaboration with the OneGeology initiative is
25 gratefully acknowledged. Thanks to the many collaborators from the LOOP team including Mark Jessell (UWA) for
26 providing the Noddy model used for the first application of the consistency-checking tool. Many thanks to
27 RING (<https://www.ring-team.org/>, last access: 6 April 2024) for academic support for use of GOCAD/SKUA
28 software, and Geoid-Solutions libraries (<https://geode-solutions.com/>, last access: 6 April 2024) for model format
29 conversions from GOCAD/SKUA (Model3D) to VTK. Use of Leapfrog Geo graciously provided by Seequent.
30 Finally, we graciously thank all our reviewers; Rob Harrap, Sam Thiele and Michel Perrin, for taking the time to
31 improve our work. This paper is NRCAN contribution number 20230104.

33 **References**

- 34 Allen, J. F.: Maintaining knowledge about temporal intervals, *Commun. ACM*, 26, 832–843, 1983.
- 35 Alsop, G.I., and Holdsworth, R.E.: Vergence and facing patterns in large scale sheath folds. *J. Struct. Geol.* 21,
36 1335-1349, 1999.
- 37 Annen, C.: Implications of incremental emplacement of magma bodies for magma differentiation, thermal aureole
38 dimensions and plutonism–volcanism relationships, *Tectonophysics*, 500 (1-4), 3-10,
39 <https://doi.org/10.1016/j.tecto.2009.04.010>, 2011.
- 40 Arora, H.; Langenhan, C., Petzold, F., Eisenstadt, V., and Althoff, K.-D.: METIS-GAN: An approach to generate
41 spatial configurations using deep learning and semantic building models, in: *ECPPM 2021–eWork and*
42 *eBusiness in Architecture, Engineering and Construction*, pp. 535 268–273, CRC Press, 2021.
- 43 Aubry, M.P, Berggren, W.A., Van Couvering, J.A. and Steininger, F.: Problems in chronostratigraphy: stages,
44 series, unit and boundary stratotypes, global stratotype section and point and tarnished golden spikes, *Earth-*
45 *Sci. Rev.*, 46, (1–4), 99-148, ISSN 0012-8252, [https://doi.org/10.1016/S0012-8252\(99\)00008-2](https://doi.org/10.1016/S0012-8252(99)00008-2), 1999.

- 1 Bai, H., Montési, L.G.J. and Behn, M.D.: MeltMigrator: A MATLAB-based software for modeling three-
2 dimensional melt migration and crustal thickness variations at mid-ocean ridges following a rules-based
3 approach, *Geochem. Geophys. Geosy.*, 18, 445–456, <https://doi.org/10.1002/2016GC006686>, 2017.
- 4 Banerjee, P. K., Banerjee, P. K., and Butterfield, R.: *Boundary element methods in engineering science*, McGraw-
5 Hill (UK), 1981.
- 6 Bertoncello, A., Sun, T., Li, H. Mariethoz, G. and Caers, J.: Conditioning Surface-Based Geological Models to Well
7 and Thickness Data. *Math. Geosci.*, 45, 873–893, <https://doi.org/10.1007/s11004-013-9455-4>, 2013.
- 8 Bezhanishvili, N., Ciancia, V., Gabelaia, D., Grilletti, G., Latella, D. and Massink, M.: Geometric Model Checking
9 of Continuous Space, *Log. Meth. Comput. Sci.*, 18, 7:1–7:38, [https://doi.org/10.46298/lmcs-18\(4:7\)2022](https://doi.org/10.46298/lmcs-18(4:7)2022),
10 2022
- 11 Bond, C.E.: Uncertainty in structural interpretation: Lessons to be learnt, *J. Struct. Geol.*, 74, 185-200,
12 <https://doi.org/10.1016/j.jsg.2015.03.003>, 2015.
- 13 Botella, A., Lévy, B. and Caumon, G.: Indirect unstructured hex-dominant mesh generation using tetrahedra
14 recombination, *Comput. Geosci.*, 20, 437–451, <https://doi.org/10.1007/s10596-015-9484-9>, 2016.
- 15 Braid, I.C.: *The Synthesis of Solids Bounded by Many Faces*, *Comm. ACM*, 18, 209-216, 1975.
- 16 Brodaric, B.: Characterizing and representing inference histories in geologic mapping, *Int. J. Geogr. Inf. Sci.*, 26 (2),
17 265-281, <https://doi.org/10.1080/13658816.2011.585992>, 2012.
- 18 Brodaric, B. and Richard, S. M.: *The GeoScience Ontology reference*. Geological Survey of Canada, Open File,
19 8796, 34. <https://doi.org/10.4095/328296>, 2021.
- 20 Brodaric, B. and Gahegan, M.: Representing Geoscientific Knowledge in Cyberinfrastructure: challenges,
21 approaches and implementations. In: Sinha, A.K. (Ed.), *Geoinformatics, Data to Knowledge*, *Geol. Soc. Am.*
22 *Spec. Pap.*, 397, 1-20. [https://doi.org/10.1130/2006.2397\(01\)](https://doi.org/10.1130/2006.2397(01)), 2006.
- 23 Brodaric, B., Gahegan, M., and Harrap, R.: The art and science of mapping: Computing geological categories from
24 field data, *Comput. Geosci.*, 30, 719-740, <https://doi.org/10.1016/j.cageo.2004.05.001>, 2004.
- 25 Burch, T.K.: Data, Models, Theory and Reality: The Structure of Demographic Knowledge. In: Billari, F.C.,
26 Prskawetz, A. (eds) *Agent-Based Computational Demography*. *Contributions to Economics. Physica*,
27 *Heidelberg*, https://doi.org/10.1007/978-3-7908-2715-6_2, 2003.
- 28 Burns, K.L.: Analysis of geological events, *Math. Geol.*, 7, 295–321, 1975.
- 29 Burns, K. L.: Lithologic topology and structural vector fields applied to subsurface prediction in geology,
30 *Proceedings of International GIS/LIS'88 accessing the World*, Third Annual International Conference, San
31 Antonio, Texas, USA, 26–34, 1988.
- 32 Burns, K.L., Shepherd, J. and Marshall, B.: Analysis of Relational Data from Metamorphic Tectonites: Derivation of
33 Deformation Sequences from Overprinting Relations, *Proceedings of the International Association for*
34 *Mathematical Geology (IAMG) 25th International Congress in Sydney, Australia, August 1976*, In: *Recent*
35 *Advances in Geomathematics, An International Symposium*, Edited by D.F. Merriam, Syracuse University,
36 *Computers and Geology Volume 2*, 171-199., 1978.
- 37 Burns, K.L. and Remfry, J.G.: A Computer Method of Constructing Geological Histories from Field Surveys and
38 Maps, *Comput. Geosci.*, 2, 141-162, 1976.
- 39 Burns, K.L., Marshall, B. and Gee, R.D.: Computer-Assisted Geological Mapping, *Proceedings of the Australian*
40 *Institute of Mining and Metallurgy*, 323, 41-47, 1969.

- 1 Cherpeau, N., Caumon, G., and Lévy, B.: Stochastic simulations of fault networks in 3-D structural modelling: C. R.
2 Geosci., **342**, 687–694, 2010.
- 3 Claramunt, C. and Jiang, B.: An integrated representation of spatial and temporal relationships between evolving
4 regions, *J. Geogr. Syst.*, 3, 411–428, 2001.
- 5 Crossley, M. D.: *Essential topology*, Springer-Verlag, London, 226 pp, ISBN 1-85233-782-6, 226, 2005.
- 6 de la Varga, M., Schaaf, A., and Wellmann, F.: GemPy 1.0: open-source stochastic geological modeling and
7 inversion, *Geosci. Model Dev.*, 12, 1–32, <https://doi.org/10.5194/gmd-12-1-2019>, 2019.
- 8 de la Varga, M., and Wellmann, J.F.: Structural geologic modeling as an inference problem: A Bayesian perspective,
9 *Interpretation*, 4, SM1-SM16, <http://dx.doi.org/10.1190/INT-2015-0188.1>, 2016.
- 10 de Kemp, E.A.: Truth Tables for consistency-checking 3D geological models, Zenodo,
11 <https://doi.org/10.5281/zenodo.13948382> , 2024.
- 12 de Kemp, E. A., Jessell, M. W., Aillères, L., Schetselaar, E. M., Hillier, M., Lindsay, M. D., and Brodaric, B.: Earth
13 model construction in challenging geologic terrain: Designing workflows and algorithms that makes sense, in:
14 *Proceedings of Exploration'17: Sixth DMEC – Decennial International Conference on Mineral Exploration*,
15 edited by: Tschirhart, V. and Thomas, M. D., *Integrating the Geosciences: The Challenge of Discovery*,
16 Toronto, Canada, 21–25 October 2017, 419–439, 2017.
- 17 de Kemp, E.A., Schetselaar, E.M., Hillier, M.J., Lydon, J.W. and Ransom, P.W.: Assessing the Workflow for
18 Regional Scale 3D Geological Modelling: An Example from the Sullivan Time Horizon, Purcell
19 Anticlinorium East Kootenay Region, Southeastern British Columbia, *Interpretation*, Special section: Building
20 complex and realistic geologic models from sparse data, 4(3), p. SM33-SM50, 2016.
- 21 de Kemp, E. A., Sprague, K., and Wong, W.: Interpretive Geology with Structural Constraints: An introduction to
22 the SPARSE © plug-in, Americas GOCAD User Meeting, Houston Texas, 1–16,
23 <https://doi.org/10.5281/zenodo.4646210>, 1 November 2004.
- 24 Deutsch, C.V.: All Realizations All the Time, In: Daya Sagar, B., Cheng, Q., Agterberg, F. (eds) *Handbook of*
25 *Mathematical Geosciences*. Springer, Cham. https://doi.org/10.1007/978-3-319-78999-6_7, 2018.
- 26 Dutranois, A., Wan-Chiu, L., Dulac, J-C, Lecomte, J-F, Callot, J-P and Rudkiewicz, J-L: Breakthrough in basin
27 modeling using time/space frame, *Offshore*, 70, 2010.
- 28 Egenhofer, M.J.: A formal definition of binary topological relationships, In: Litwin, W., Schek, HJ. (eds)
29 *Foundations of Data Organization and Algorithms*, FODO 1989, *Lecture Notes in Computer Science*,
30 Springer, Berlin, Heidelberg, 367, https://doi.org/10.1007/3-540-51295-0_148, 1989.
- 31 Egenhofer, M., Sharma J. and Mark D.: A critical comparison of the 4-intersection and 9- intersection models for
32 spatial relations: formal analysis, In: R. McMaster and M. Armstrong (eds), *Autocarto 11*, Minneapolis, MN,
33 1-11, 1993.
- 34 Egenhofer, M. and Franzosa, R., 1991. Point-set topological relations, *Int. J. Geogr. Inf. Syst.*, 5, 161-174.
- 35 Fattah, M.: *Physical Geology*, On line course, UDEMY, (<https://www.udemy.com/course/geology-fundamentalz/>,
36 last access: 6 April 2024), 2022.
- 37 Finkl C.W., *Field Geology*. In: Finkl C. (eds) *Applied Geology*. *Encyclopedia of Earth Sciences Series*, vol 3.
38 Springer, Boston, MA. https://doi.org/10.1007/0-387-30842-3_21, 1984.
- 39 Fossen H., *Structural Geology*. Cambridge University Press, New York, 524, 2016.

- 1 Frank, T.: Advanced visualization and modeling of tetrahedral meshes. Thèse de doctorat dirigée par Mallet, Jean-
2 Laurent Géosciences Vandoeuvre-les-Nancy, INPL 2006. <http://www.theses.fr/2006INPL015N>, 2006
- 3 Frodeman, R.: Geological reasoning: geology as an interpretive and historical science, *Geol. Soc. Am. Bull.*, 107,
4 960-968, 1995.
- 5 Galton, A.: Spatial and temporal knowledge representation, *Earth Sci. Inform.*, 2, 169–187,
6 <https://doi.org/10.1007/s12145-0090027-6>, 2009.
- 7 Geodes-Solutions, <https://geode-solutions.com/opengeode/>, last access: 10 Sept. 2024).
- 8 Garcia, L.F., Abel, M., Perrin, M., and dos Santos Alvarenga, R.: The GeoCore ontology: A core ontology for
9 general use in Geology, *Comput. Geosci.*, 135, 104387, <https://doi.org/10.1016/j.cageo.2019.104387>, 2020
- 10 Giraud, J., Caumon, G., Grose, L., Ogarko, V., and Cupillard, P.: Integration of automatic implicit geological
11 modelling in deterministic geophysical inversion, *Solid Earth*, 15, 63–89, [https://doi.org/10.5194/se-15-63-](https://doi.org/10.5194/se-15-63-2024)
12 [2024](https://doi.org/10.5194/se-15-63-2024), 2024.
- 13 Giraud, J., Lindsay, M., Jessell, M., and Ogarko, V.: Towards plausible lithological classification from geophysical
14 inversion: honouring geological principles in subsurface imaging, *Solid Earth*, 11, 419–436,
15 <https://doi.org/10.5194/se-11-419-2020>, 2020.
- 16 Grose, L., Ailleres, L., Laurent, G., Armit, R., and Jessell, M.: Inversion of geological knowledge for fold geometry,
17 *J. Struct. Geol.*, 119, 1–14, <https://doi.org/10.1016/j.jsg.2018.11.010>, 2019.
- 18 Gleeson, T., Wagener, T., Döll, P., Zipper, S. C., West, C., Wada, Y., Taylor, R., Scanlon, B., Rosolem, R.,
19 Rahman, S., Oshinlaja, N., Maxwell, R., Lo, M.-H., Kim, H., Hill, M., Hartmann, A., Fogg, G., Famiglietti, J.
20 S., Ducharme, A., de Graaf, I., Cuthbert, M., Condon, L., Bresciani, E., and Bierkens, M. F. P.: GMD
21 perspective: The quest to improve the evaluation of groundwater representation in continental- to global-scale
22 models, *Geosci. Model Dev.*, 14, 7545–7571, <https://doi.org/10.5194/gmd-14-7545-2021>, 2021.
- 23 Gong, P. and Mu, L.: Error detection through consistency checking, *Geogr. Inf. Sci.*, 6, 188–193, 2000.
- 24 Groshong, R. H. Jr.: 3-D Structural Geology a Practical Guide to Quantitative Surface and Subsurface Map
25 Interpretation, (2nd Edition), Springer-Verlag Berlin Heidelberg, ISBN-13, 978-3540310549, 2006.
- 26 Harrap, R.: A Legend Language for Geologic Maps, Precambrian Times, Geological Association of Canada,
27 Precambrian Division Newsletter, Volume 1, Issue 1, Jan./Feb. 2001, p.1, 3-9, 2001.
- 28 Hillier, M. J., Schetselaar, E. M., de Kemp, E. A., and Perron, G.: Three-dimensional modelling of geological
29 surfaces using generalized interpolation with radial basis functions, *Math. Geosci.*, 46, 931–953, 2014.
- 30 Hillier, M., de Kemp, E. A., and Schetselaar, E. M.: Implicitly modelled stratigraphic surfaces using generalized
31 interpolation, in: AIP conference proceedings, 1738, 050004, International Conference of Numerical Analysis
32 and Applied Mathematics, 22–28 September 2015, Rhodes, Greece, <https://doi.org/10.1063/1.4951819>, 2016.
- 33 Hillier, M. J., Wellmann, F., Brodaric, B., de Kemp, E. A., and Schetselaar, E.: Three-Dimensional Structural
34 Geological Modeling Using Graph Neural Networks, *Math. Geosci.*, [https://doi.org/10.1007/s11004-021-](https://doi.org/10.1007/s11004-021-09945-x)
35 [09945-x](https://doi.org/10.1007/s11004-021-09945-x), 2021.
- 36 Hillier, M.J., Schetselaar, E. M., de Kemp, E. A.: SURFE implicit code library repository, (Open Source),
37 <https://github.com/MichaelHillier/surfe>, (last access: 6 April 2024), 2021.
- 38 Hinojosa, J.H. and Mickus, K.L.: Foreland basin-a FORTRAN program to model the formation of foreland basins
39 resulting from the flexural deflection of the lithosphere caused by a time-varying distributed load, *Comput.*
40 *Geosci.*, 19(9), 1321-1332, [https://doi.org/10.1016/0098-3004\(93\)90032-Z](https://doi.org/10.1016/0098-3004(93)90032-Z), 1993.

- 1 Hobbs, B., Regenauer-Lieb, K. and Ord, A.: Thermodynamics of Folding in the Middle to Lower Crust, *Geology*, 35
2 (2), 175-178, <https://doi.org/10.1130/G23188A.1>, 2007.
- 3 Jayr, S., Gringarten, E., Tertois, A.-L., Mallet, J.-L. and Dulac, J.-C.: The need for a correct geological modelling
4 support: The advent of the UVT-transform, *First Break*, 26, 73-79, [https://doi.org/10.3997/1365-](https://doi.org/10.3997/1365-2397.26.10.28558)
5 [2397.26.10.28558](https://doi.org/10.3997/1365-2397.26.10.28558), 2008.
- 6 Jessell, M. W.: Noddy: an interactive map creation package, Unpublished MSc Thesis, University of London, 1981.
- 7 Jessell, M., Ogarko, V., de Rose, Y., Lindsay, M., Joshi, R., Piechocka, A., Grose, L., de la Varga, M., Aillères, L.,
8 and Pirot, G.: Automated geological map deconstruction for 3D model construction using map2loop 1.0
9 and map2model 1.0, *Geosci. Model Dev.*, 14, 5063–5092, <https://doi.org/10.5194/gmd-14-5063-2021>, 2021.
- 10 Jessell, M. W., Aillères, L. and de Kemp, E. A.: Towards an Integrated Inversion of Geoscientific data: what price
11 of Geology? *Tectonophysics*, 490(3-4), 294-306, 2010.
- 12 Jessell, M., Aillères, L., de Kemp, E.A., Lindsay, M., Wellmann, J., Hillier, M., Laurent, G., Carmichael, T., and
13 Martin, R.: Next generation three-dimensional geologic modeling and inversion, *Soc. Eco. Geo. Spc. Pub.*, 18,
14 261–272, 2014.
- 15 Kardel, T. and Paul Maquet, P.: Nicolaus Steno: Biography and Original Papers of a 17th Century Scientist, 2013'th
16 (Kindle) Edition, Springer; 2013th edition, 739, ISBN-13 978-3642250781, 2012.
- 17 Lajevardi, S. and Deutsch, C.V.: Stochastic regridding of geological models for flow simulation, *B. Can. Petrol.*
18 *Geol.*, 63: 374–392, <https://doi.org/10.2113/gscpgbull.63.4.374>, 2015.
- 19 Lajaunie, C., Courrioux, G., and Manuel, L.: Foliation fields and 3D cartography in geology: principles of a method
20 based on potential interpolation. *Math. Geol.*, 29:571–584, <https://doi.org/10.1007/BF02775087>, 1997.
- 21 Le, H.H., Gabriel, P., Gietzel, J. and Schaeben, H.: An object-relational spatio-temporal geoscience data model,
22 *Comput. Geosci.*, 57, 104-115, ISSN 0098-3004, <https://doi.org/10.1016/j.cageo.2013.04.014>, 2013.
- 23 Lindsay, M.D., Aillères, L., Jessell, M.W., de Kemp, E.A., Betts, P.G.: Locating and quantifying geological
24 uncertainty in three-dimensional models: Analysis of the Gippsland Basin, southeastern Australia,
25 *Tectonophysics*, 546-547, 10-27, <https://doi.org/10.1016/j.tecto.2012.04.007>, 2012.
- 26 Lyell, (Sir) C.: Principles of Geology: Or, the Modern Changes of the Earth and Its Inhabitants, Considered As
27 Illustrative of Geology, Legare Street Press, ISBN-13 978-1015539976, 496, (original 1833) 2022.
- 28 Mallet, J-L.: Space–Time Mathematical Framework for Sedimentary Geology. *Math. Geol.*, 36, 1–32,
29 <https://doi.org/10.1023/B:MATG.0000016228.75495.7c>, 2004.
- 30 Mallet, J-L., Jacquemin, P. and Cheimanoff, N.: GOCAD project: Geometric modeling of complex geological
31 surfaces, in: SEG Technical Program Expanded Abstracts, 126-128, <https://doi.org/10.1190/1.1889515>, 1989.
- 32 Maxelon, M, Renard, P., Courrioux, G., Brändli, M. and Mancktelow, N.: A workflow to facilitate three-
33 dimensional geometrical modelling of complex poly-deformed geological units, *Comput. Geosci.*, 35(3), 644-
34 658, <https://doi.org/10.1016/j.cageo.2008.06.005>, 2009.
- 35 McKay, G. and Harris, J.R.: Comparison of the Data-Driven Random Forests Model and a Knowledge-Driven
36 Method for Mineral Prospectivity Mapping: A Case Study for Gold Deposits Around the Huritz Group and
37 Nueltin Suite, Nunavut, Canada. *Nat. Resour. Res.*, 25, 125–143. <https://doi.org/10.1007/s11053-015-9274-z>,
38 2016.
- 39 McMechan, M.E., Root, K.G., Simony, P.S. and Pattison, D.R.M.: Nailed to the craton: Stratigraphic continuity
40 across the southeastern Canadian Cordillera with tectonic implications for ribbon continent models, *Geology*,
41 49(1): 101–105, <https://doi.org/10.1130/G48060>, 2021.

- 1 Melnikova, Y., Cordua, K. S., and Mosegaard, K.: History Matching: Towards Geologically Reasonable Models.
2 Abstract from EAGE Integrated Reservoir Modelling: Are we doing it right?, Dubai, United Arab Emirates,
3 2012.
- 4 Michalak, J.: Topological conceptual model of geological relative time scale for geoinformation systems, *Comput.*
5 *Geosci.*, 31-7, 865-876, ISSN 0098-3004, <https://doi.org/10.1016/j.cageo.2005.03.001>, 2005.
- 6 Morley, C.K.: Out-of-sequence thrusts, *Tectonics*, 7 (3), 539-561, 1988.
- 7 New South Wales (NSW), Australia, Department of Primary Industries (DPI), History of Geology, February 2007,
8 Primefacts 563, 6,
9 ([https://digs.geoscience.nsw.gov.au/api/download/c6ae94e9dc65f614492646c269ea3731/Primefact_563_Minif](https://digs.geoscience.nsw.gov.au/api/download/c6ae94e9dc65f614492646c269ea3731/Primefact_563_Minifact_60_History_of_geology.pdf)
10 [act_60_History_of_geology.pdf](https://digs.geoscience.nsw.gov.au/api/download/c6ae94e9dc65f614492646c269ea3731/Primefact_563_Minifact_60_History_of_geology.pdf), last access: 20 April 2022).
- 11 Nikoohemat, S., Diakit , A. A., Lehtola, V., Zlatanova, S., and Vosselman, G.: Consistency grammar for 3D indoor
12 model checking, *Trans. GIS*, 25, 189–212, <https://doi.org/10.1111/tgis.12686>, 2021.
- 13 Pellerin, J., Caumon, G., Julio, C., Mejia-Herrera, P., and Botella, A.: Elements for measuring the complexity of 3D
14 structural models: Connectivity and geometry, *Comput. Geosci.*, 76, 130-140, ISSN 0098-3004,
15 <https://doi.org/10.1016/j.cageo.2015.01.002>, 2015.
- 16 Pellerin, J., Botella, A., Bonneau, F., Mazuyer, A., Chauvin, B., L vy, B., Caumon, G.: RINGMesh: A programming
17 library for developing mesh-based geomodeling applications, *Comput. Geosci.*, 104, 93-100, ISSN 0098-3004,
18 <https://doi.org/10.1016/j.cageo.2017.03.005>, 2017.
- 19 Perrin, M., Poudret, M., Guiard, N. and Schneider, S.: Chapter 6: Geological Surface Assemblage, In: Shared Earth
20 Modeling, Knowledge driven solutions for building and managing subsurface 3D geological models, Energies
21 Nouvelles Publications - TECHNIP, Paris, France, 115-139, 2013.
- 22 Perrin, M., Morel, O., Mastella, L., and Alexandre, L.: Geological Time Formalization: an improved formal model
23 for describing time successions and their correlation, *Earth Sci. Inform.*, 4, 81–96,
24 <https://doi.org/10.1007/s12145-011-0080-9>, 2011.
- 25 Pizzella, L., Alais, R., Lopez, S., Freulon X., and Rivoirard, J.: Taking Better Advantage of Fold Axis Data to
26 Characterize Anisotropy of Complex Folded Structures in the Implicit Modeling Framework. *Math. Geosci.*,
27 54, 95–130, <https://doi.org/10.1007/s11004-021-09950-0>, 2022.
- 28 Pycrz, M. J., Sech, R. P., Covault, J. A., Willis, B. J., Sylvester, Z., Sun, T., and Garner, D.: Stratigraphic rule-based
29 reservoir modeling, *B. Can. Petrol. Geol.*, 63, 287–303, 2015.
- 30 Qu, Y., Perrin, M., Torabi, A., Abel, Giese, M.: GeoFault: A well-founded fault ontology for interoperability in
31 geological modeling, *Comput. Geosci.*, 182, 105478, <https://doi.org/10.1016/j.cageo.2023.105478>, 2024.
- 32 Ranalli, G.: A stochastic model for strike-slip faulting. *Math. Geol.*, 12, 399–412,
33 <https://doi.org/10.1007/BF01029423>, 1980.
- 34 Rauch, A. Sartori, M., Rossi, E., Baland, P. and Castellort, S.: Trace Information Extraction (TIE): A new
35 approach to extract structural information from traces in geological maps, *J. Struct. Geol.*, 126, 286-300, ISSN
36 0191-8141, <https://doi.org/10.1016/j.jsg.2019.06.007>, 2019.
- 37 Rothery, D.: *Geology: A Complete Introduction*, Quercus; 1st edition (Feb. 16 2016), ISBN-13, 978-1473601550,
38 384, 2016.
- 39 Schaaf, A., de la Varga, M., Wellmann, F., and Bond, C. E.: Constraining stochastic 3-D structural geological
40 models with topology information using approximate Bayesian computation in GemPy 2.1, *Geosci. Model*
41 *Dev.*, 14, 3899–3913, <https://doi.org/10.5194/gmd-14-3899-2021>, 2021.

- 1 Schetselaar, E. M. and de Kemp, E. A.: Topological encoding of spatial relationships to support geological
2 modelling in a 3-D GIS environment, Int. Assoc. for Mathematical Geology XIth International Congress,
3 Université de Liège - Belgium, 2006.
- 4 Shokouhi, P., Kumar, V., Prathipati, S., Hosseini, S.A., Giles, C.L., and Kifer, D.: Physics-informed deep learning
5 for prediction of CO2 storage site response, *J. Contam. Hydrol.*, 241, 103835,
6 <https://doi.org/10.1016/j.jconhyd.2021.103835>, 2021.
- 7 Thapa, P. and McMechan, M.E.: Methodology for portraying 3D structure using ArcGIS: a test case from the
8 southern Canadian Rocky Mountains, British Columbia and Alberta, Geological Survey of Canada, Open File
9 8576, <https://doi.org/10.4095/314941>, 2019.
- 10 Thiele, S. T., Jessel, M. W., Lindsay, M., Ogarko, V., Wellmann, J. F., and Pakyuz-Charrier, E.: The topology of
11 geology 1: Topological analysis, *J. Struct. Geol.*, 91, 27-38, <https://doi.org/10.1016/j.jsg.2016.08.009>, 2016a.
- 12 Thiele, S.T., Jessel, M.W., Lindsay, M., Wellmann, J.F. and Pakyuz-Charrier, E.: The topology of geology 2:
13 Topological uncertainty, *J. Struct. Geol.*, 91, 74-87, ISSN 0191-8141,
14 <https://doi.org/10.1016/j.jsg.2016.08.010>, 2016b.
- 15 van Giffen, B. Herhausen, D., and Fahse, T.: Overcoming the pitfalls and perils of algorithms: A classification of
16 machine learning biases and mitigation methods, *J. Bus. Res.*, 144, 93-106, ISSN 0148-2963,
17 <https://doi.org/10.1016/j.jbusres.2022.01.076>, 2022.
- 18 Van Oosterom, P.: Maintaining consistent topology including historical data in a large spatial database, 13, 327–
19 336, 1997.
- 20 von Harten, J., de la Varga, M., Hillier, M., and Wellmann, F.: Informed Local Smoothing in 3D Implicit Geological
21 Modeling, *Minerals*, 11, 1281, <https://doi.org/10.3390/min11111281>, 2021.
- 22 Wellmann, F. and Caumon, G.: 3-D Structural geological models: Concepts, methods, and uncertainties, *Adv.*
23 *Geophys.*, pp. 1–121, <https://doi.org/10.1016/bs.agph.2018.09.001>, 2018.
- 24 Zhan, X., Lu, C. and Hu, G.: A Formal Representation of the Semantics of Structural Geological Models, *Sci.*
25 *Program.*, 5553774, <https://doi.org/10.1155/2022/5553774>, 2022.
- 26 Zhan, X., Liang, J., Lu, C., and Hu, G.: Semantic Description and Complete Computer Characterization of Structural
27 Geological Models, *Geoscientific Model Development Discussions*, 1–39, 2019.
- 28 Ziggelaar, A.: The age of Earth in Niels Stensen's geology, *Geol. Soc. Am. Mem.*, 203, 135-142, 2009.
- 29 Zlatanova, S., Rahman, A. A., and Shi, W.: Topological models and frameworks for 3D spatial objects, *Comput.*
30 *Geosci.*, 30, 419–428, 2004.
- 31